

# Solving the Security Constrained Unit Commitment problem: three novel approaches

Alessandro Francesco Castelli, Iiro Harjunoski, Jan Poland, Marco Giuntoli, Emanuele Martelli, Ignacio Grossmann

## Abstract

This work proposes three novel approaches to speed up the solution of the Security Constrained Unit Commitment problem: an improvement of an active-set iterative approach taken from literature, an approach using solver callback functions for the evaluation of system and security constraints in the branch-and-bound tree, and one based on a shrinking horizon decomposition integrated with the use of callback functions. The three approaches were tested over five different case studies and compared against an approach taken from literature to assess scalability and performance. Results show that the modified iterative approach is always faster than the original one reported in the literature (between -58% and -93% run time), while the callback-based method does not reduce the computational time of large-scale instances. Finally, the shrinking-horizon-based approach was proved to be the fastest (up to -98% less time) despite not guaranteeing optimality (about 1% suboptimal).

## Keywords

Unit Commitment, Optimization, Decomposition, N-1 reliability, Grid Operation

## Nomenclature

---

### *Abbreviations*

---

AC	Alternating Current
DC	Direct Current
ED	Economic Dispatch
ISF	Injection Shifting Factor
LODF	Line Outage Distribution Factor
LSF	Linear Sensitivity Factor
O&M	Operation and Maintenance
PTDF	Power Transfer Distribution Factor
QP	Quadratic Programming
SCUC	Security Constrained Unit Commitment
SSNC	System and Security Network Constraint
TSO	Transmission System Operator

---

### *Sets*

---

$\Gamma', \Gamma''$	Sets of the active system and security network constraints
---------------------	--

$B$	Set of the buses in the network
$G$	Set of the available generators
$G^{on}$	$G^{on} \subseteq G$ , set of the must-run generators
$G^{off}$	$G^{off} \subseteq G$ , set of generators currently not available
$G_r^R$	$G_r^R \subseteq G$ , set of the generators belonging to reserve area $r$
$G_b^B$	$G_b^B \subseteq G$ , set of the generators connected directly to bus $b$
$L$	Set of the transmission lines
$L_b^{in}, L_b^{out}$	$L_b^B \subseteq L$ , set of the transmission lines connected to bus $b$ (in- and out-going)
$L^{off}$	$L^{off} \subseteq L$ , set of the transmission lines currently not available
$R$	Network reserve areas
$T$	Set of the timesteps within the horizon considered

### Binary Variables

$\delta_{i,t}^{on}, \delta_{i,t}^{off}$	Start-up/shut-down flagger for unit $i$ at time $t$ . 1 if unit $i$ started-up/shut-down at $t$ , 0 otherwise
$z_{i,t}$	On/off status of unit $i$ at time $t$ . 1 if unit $i$ is on at time $t$ , 0 otherwise.

### Continuous Variables

$d_{b,t}^{shed}$	Demand shed at bus $b$ at time $t$ [MWh]
$f_{c,t}$	Pre-outage power flowing through line $c$ at time $t$ [MW]
$f_{c,t}^d$	Post-outage power flowing through line $c$ at time $t$ resulting from outage of line $d$ [MW]
$f_{c,t}^{d,QP}$	Post-outage power flowing through line $c$ at time $t$ resulting from outage of line $d$ in the QP subproblem [MW]
$f_{c,t}^{QP}$	Pre-outage power flowing through line $c$ at time $t$ in the QP subproblem [MW]
$p_{i,t}$	Energy generated by unit $i$ at time $t$ [MWh]
$p_{i,t}^{QP}$	Generation that unit $i$ at time $t$ should have to meet the considered SSNCs in the QP subproblem [MWh]
$r_{i,t}^{up}, r_{i,t}^{down}$	Upward and downward reserve quantities made available by unit $i$ at time $t$ [MWh]

### Parameters

$\#RU_i, \#RD_i$	Minimum number of timesteps of length $dt$ required by unit $i$ to go from minimum/maximum to maximum/minimum generation according to the ramping limit $RU_i/RD_i$
$\#SU_i, \#SD_i$	Minimum number of timesteps needed by unit $i$ to ramp up from $SU_i$ to the maximum generation / to ramp down from maximum generation to $SD_i$
$\Delta t^{adv}$	Time advancement of the shrinking horizon algorithm (equal to the number of discrete timesteps considered in each shrunk horizon)
$c_{i,t}, c_i^{on}, c_i^{su}, c_i^{sd}$	Variable [\$/MWh], fixed hourly [\$/h], stat-up [\$/start-up] and shut-down [\$/shut-down] operational costs for unit $i$
$c^{shed}$	Virtual cost related to shed load [\$/MWh]

$c_{b,t}^d$	Virtual revenue linked to the amount of demand of bus $b$ at time $t$ that is met [\$/MWh]
$D_{b,t}$	Demand related to a timestep duration $dt$ to meet at bus $b$ at time $t$ [MWh]
$D_{b,t}^{agg}$	Demand related to the aggregate timestep $t$ (of duration $\tilde{t} \cdot dt$ ) to meet at bus $b$ [MWh]
$dt$	Timestep duration [h]
$\bar{F}_c$	Maximum power flow allowed through line $c$ [MW]
$H_i^U, H_i^D$	Number of time periods for completing the minimum up/down time at the beginning of the considered time horizon, for unit $i$
$\underline{P}_i, \bar{P}_i$	Minimum and maximum allowed generation unit $i$ within $dt$ [MWh]
$RU_i, RD_i$	Ramp-up/down limits for unit $i$ between timesteps of duration $dt$ [MWh]
$Res_{r,t}^{up}, Res_{r,t}^{down}$	Upward and downward reserve requirements of area $r$ at time $t$ [MWh]
$SU_i, SD_i$	Ramping limits at start-up/shutdown for unit $i$ for timestep duration $dt$ [MWh]
$\tilde{t}$	Number of original timesteps considered in the aggregated one.
$UT_i, DT_i$	Minimum required number of timesteps of duration $dt$ that unit $i$ is required to stay on/off before being shutdown/started-up
$\widetilde{UT}_{i,t}, \widetilde{DT}_{i,t}$	Minimum required number of timesteps (aggregate and/or discrete) that unit $i$ is required to stay on/off in the timesteps before $t$ ( $t$ included), if on/off at $t$
$\widetilde{UT}_i^{agg}, \widetilde{DT}_i^{agg}$	Minimum required number of timesteps (aggregate and/or discrete) that unit $i$ is required to stay on/off starting up/shutting down at the beginning of the horizon
$y_c$	$y: c \rightarrow (m, n)$ , map defining the link between line $c$ and the connected buses $m$ and $n$

---

## 1. Introduction

In the last two decades many changes have happened to electricity markets worldwide, mainly due to deregulation. This opened the markets to many operators in the power sector, providing competition and lowering the energy costs. However, this increased participation made grid operation more challenging for Independent System Operators (ISOs). This is because the ISO is in charge of determining the optimal operational scheduling of every generator connected to the grid for a fixed time horizon, with the aim of minimizing the total operational cost of satisfying the demand at each bus (consumption point). The resulting decisions must comply with the generators' operational constraints, as well as with those related to the transmission system (e.g., no lines overload). In addition, N-1 reliability is enforced by guaranteeing that no line will be overloaded under any contingency in which at most one of them is out of service. What we have described is known in the literature as the Security Constrained Unit Commitment (SCUC) problem [1] and it is characterized by high combinatorial complexity, requiring the development of special-purpose mathematical optimization tools for its solution.

The mathematical optimization model involves both linear and non-linear equations describing the generators performance and the AC nature of the grid. This, together with the N-1 reliability consideration in the problem, makes the model hard to solve. One of the first works proposing a method to solve the AC SCUC problem is the one by Fu et al. [2]. In this work the original problem is split into a master and a sub-problem, that are solved iteratively. Lagrangean relaxation and Dynamic Programming are used for solving the master problem, while the subproblem finds the solution of the Optimal Power Flow (OPF) problem and checks if any of the system and security constraints are violated. If so, Benders cuts are added to the master problem, corresponding to the violations found. A more recent work proposed by Gupta et al. [3] relies on a similar concept: Generalized Benders Decomposition is used to solve the MINLP model the AC SCUC problem by formulating a MIQP master problem and an NLP subproblem. As before, the NLP subproblem is used for the evaluation of the violated network constraints to be added to the master problem. Dipan Biswas et al. [4] showed how their two-stage algorithm solving an MILP and an NLP problem sequentially proved to be yield solutions that are only 2% worse than the solution of the original problem. Another work focusing on the loss of optimality associated to model linearization can be found in Jiang et al.[5], where different linearized models are considered and compared.

A methodology based on Ordinal Optimization [6] was proposed by Nan et al. [7]. This iterative approach resembles in the sequential solution of an approximated and detailed model, with the aim to find a “good” solution rather than the optimal one. In the single test case considered it was shown that the computational time was significantly reduced compared to Benders Decomposition, while providing a similar solution.

A tri-level decomposition approach was proposed by Amjady et al. [8], based on finding the unit commitment considering AC line constraints and wind generation worst-case scenario. The methodology proved to be effective in finding a robust solution for the small test case considered, but scalability was not assessed.

As it can be seen, the computational burden associated with solving the original AC SCUC is characterized by the small test instances (e.g., 24, 118 bus systems) considered in the previously cited studies. This gives rise to the need of problem linearization and decomposition. Moreover, most of the works focused on solving the AC SCUC problem consider simple test cases, not providing evidence of the applicability to real world case studies. Furthermore, they are significantly slower than current methods.

For this reason, today’s state of the art consists of solving the linearized version of the SCUC problem. The resulting DC SCUC problem is described by means of an MILP model that is easier to solve. The non-linear security and network constraints are substituted by linear inequalities described by sensitivity coefficients that are grouped in the Power Transfer Distribution Factors (PTDF) and Line Outage Distribution Factors (LODF) matrices. For a DC system, the PTDF matrix describes how the power supplies/withdrawn to/from each bus flows across each line, while the LODF matrix described how the power flowing on a certain line is diverted on the others in case of contingency. Different methods for the evaluation of these matrices can be found in the literature, aiming at improving the computational performance during their computation (e.g., [9], [10] and [11]) or at describing more complex systems comprising both AC and DC lines (see [12] for an example).

Despite the reduction in the computational burden achieved by considering the DC SCUC problem, the model still features a large number of system and security constraints (e.g., the number of N-1 security constraints is equal to the number of system’s lines squared). This makes

the problem difficult to solve due to the memory requirements associated with the model size, therefore highlighting the need of developing special purpose solution approaches to address the problem. In their work, Xavier et al. [13] proposed an iterative approach that consists of solving an initial MILP problem with no system and security constraints, evaluating the OPF based on the resulting injections, checking constraint violation and adding them to the model. In this way only the active network constraints are added to the model, which is a smaller subset, and therefore requires significantly less memory. While in this method the new active constraints are “learned” as new solutions are evaluated, other approaches are used to filter out in advance the active constraints. In a different work [14] the same authors proposed different machine learning tools for the prediction of the active network constraints and a starting solution based on past, optimal instances. This data driven approach was able to decrease the size of the problem, while speeding up the solution time, while still guaranteeing optimality. Other similar approaches have been developed with the aim of predicting the correct pool of active constraints so as to avoid any redundancy. More recent approaches propose other data-driven filtering methods to improve the overall solution time. Yang et al. [15] used stacked denoising autoencoders (deep neural network used for dimensionality reduction) during the training phase to evaluate the non-linear relationship between active constraints and the operational solutions. An expanded sequence-to-sequence (E-Seq2Seq)-based data-driven SCUC expert system for dynamic multiple-sequence mapping samples is proposed by Yang et al. [16], with the aim of providing a solution to the SCUC problem based on trained data and avoiding the optimization process.

Other, non-data-driven approaches can be found in the literature as well, like the cost-driven screening method proposed by Porras et al. [17] where valid inequalities are introduced to tighten the feasible region of the relaxed SCUC LP problem. The relaxed solution is then used for evaluating the active constraints and discard the redundant ones, thus being independent from any training phase (unlike the previous methods). As a general statement, many works in the literature show how applying these constraint filtering approaches to iterative solution methods can significantly reduce the computational time.

Finally, some well-known works address the issue of solving the SCUC under uncertainty (e.g., due to the increased penetration of non-dispatchable renewable energy sources). For example, Wang et al. [18] propose an iterative approach to solve a two-stage stochastic SCUC with different forecast scenarios related to wind generation. The deterministic commitment solution of the master problem is evaluated over a set of wind generation scenarios to check violations of the network constraints and Benders cuts are added if they occur. Another remarkable work by Bertsimas et al. [19] proposes an adaptive robust optimization model for solving the SCUC problem. The two-level method is based on a Benders decomposition type algorithm that is able to evaluate a robust solution for any realization of the uncertain demands at each bus within a predefined, deterministic uncertainty set. In another paper by Wang et al. [20] an ad-hoc decomposition algorithm is proposed for the parallel solution of a stochastic SCUC characterized by uncertain renewable energy generation. Lagrangean decomposition is applied for solving the stochastic problems where the uncertain parameters are the generators and lines’ reliability. In the work by Wu et al. [21], the authors consider line outage scenarios instead of the N-1 constraints, thus building a large scenario tree.

Despite their capability of including the uncertainties of the parameters in the problem, the approaches above mentioned require long computational times, which is not suitable for industrial practice (ISOs usually need to update the generators’ schedule multiple times throughout the day, e.g., on an hourly basis). Given this requirement, and by considering that updating the solution

frequently is an effective method to cope with forecast uncertainty, effort should be placed in solving the DC SCUC problem as quickly as possible. One way to achieve this is by adopting data-driven network constraints filtering tools (as the ones cited before), since they have proven to be effective on relatively small test cases. However, they require large dataset for the training phase. Since for large systems this data is either not available or the evaluation of optimal solutions requires a long time (sometimes the problem is even intractable), this approach might become impractical.

For these reasons, this work proposes three novel solution approaches aimed at improving the solution time of the DC SCUC problem. The first one is an improvement of the method presented in Xavier et al. [13], the second one consists of the use of solver callback functions for the addition of the network constraints as Lazy Constraints to the model (similar to what done by Liu et al. in [22]), and the last one is a Shrinking Horizon algorithm (similar to approaches found in stochastic Model Predictive Control [23] and scheduling [24] problems) featuring callback functions for contingency and system constraint discovery. Contrary to the previously mentioned data-driven methods (which largely rely on Machine Learning), the ones proposed in this work are based on modern optimization-based approaches that do not make them dependent on training datasets while guaranteeing the feasibility of the predicted solutions. The three novel features of the proposed methods are: (a) using a more sophisticated constraint filtering method that is able to reduce the computational time needed by the new iterative approach; (b) embedding the filtering approach within the solver's branch-and-cut algorithm; (c) reducing the size of the problem while guaranteeing feasibility.

## 2. Problem Statement

As previously mentioned, the problem addressed in this paper is known in literature as Security Constrained Unit Commitment problem, and it consists of evaluating the operational schedule of each generation unit available on the considered power grid (which unit to be turned on/off and its generation level) with the aim of meeting the demand at each bus of the network while avoiding overload on any transmission line under nominal condition, and for whichever contingency in which at most one line is out of service (N-1). The problem can be therefore stated as follows:

*Given:*

- The set of generation units and their operational parameters,
- The network topology and transmission line limits,
- The specified time horizon,
- The expected energy demand at each bus,
- The status of the units and transmission lines at the beginning of the considered time-horizon (on/off and current power generation),

*Find the optimal commitment (schedule) of the units, which minimizes the total generation cost/maximizes the net operational revenue subject to the following constraints:*

- Units' operational limits (maximum and minimum allowed load, ramping limits, minimum up- and down-times)
- Energy balances at each node
- Transmission limits on each line
- Reserve constraints
- N-1 contingency constraints

### 3. Methodology

The proposed methodology consists of two main steps: (1) the formulation of a tight and efficient MILP model for the optimal SCUC solution, (2) the design and development of ad-hoc solution approaches to reduce the computational expense of the optimization. The three different solution approaches are presented in this section: the first one is a variation of the well-known iterative method based on the active set-strategy and presented in [13], the second approach uses solver's callback functionalities for the evaluation and addition of security and safety constraints, and the third one is a Shrinking Horizon algorithm inheriting the same callback functions featured in the third approach.

#### 3.1. Mixed Integer Linear Programming model

The SCUC problem considers a linearized (DC) version of the original non-linear problem and therefore can be modelled as an MILP. The network and generation units are modelled by means of linear constraints, divided into the following four groups: generation units operational constraints, reserve constraints, energy balance constraints and network security and systems constraints. The model shares many of the features belonging to other works in literature. The duration constraints (Eqs. (2)-(7)) are taken from Morales-España et al. [25], while the ramping limits (Eqs. (8)-(11)) come from Constante-Flores et al. [26]. Finally, reserve constraints (Eqs. (14)-(23)) were formulated starting from the ones found in Tejada-Arango et al. [27].

In summary, the MILP model describing the SCUC problem is given by the constraints defined by Eqs. (1)-(32). Regarding the objective function, two are considered in this study: Eqs. (33) and (34) (see next).

#### ***Generation units' operational constraints***

The operational constraints related to each unit available in the considered grid are described in this section. At first, each unit is characterized by its maximum and minimum generation limits:

$$\underline{P}_i z_{i,t} \leq p_{i,t} \leq \bar{P}_i z_{i,t} \quad \forall i \in G, \forall t \in T \quad (1)$$

where  $\underline{P}_i$  and  $\bar{P}_i$  are the minimum and maximum allowed generation levels of unit  $i$  respectively,  $p_{i,t}$  the energy (MWh) generated by unit  $i$  at time  $t$ , and  $z_{i,t}$  the on-off status of unit  $i$  at time  $t$ .

The start-up and shutdown flags  $\delta_{u,t}^{on}$  and  $\delta_{u,t}^{off}$  are introduced to define when unit  $i$  is switched on or off. The logical relationship between the on-off status and the already mentioned flags is defined by the following constraint for all timesteps except the first one:

$$z_{i,t-1} - z_{i,t} + \delta_{i,t}^{on} - \delta_{i,t}^{off} = 0 \quad \forall i \in G \setminus G^{on}, \forall t = 2, \dots, |T| \quad (2)$$

Only for the first timestep of the horizon, the relationship takes the following form:

$$z_i^{ini} - z_{i,1} + \delta_{i,1}^{on} - \delta_{i,1}^{off} = 0 \quad \forall i \in G \setminus G^{on} \quad (3)$$

with  $z_i^{ini}$  a parameter being either equal to 0 or 1, defining the inherited initial on-off status of the considered unit.

Other time-linking constraints are those describing the minimum up- and down-times for each unit. These are taken from Morales-España et al. [28] since they correspond to the tightest formulation found in the literature (as also stated in Knueven et al. [29]). The minimum up-time is enforced by the following expression:

$$\sum_{\tau=t-UT_i+1}^t \delta_{i,\tau}^{on} \leq z_{i,t} \quad \forall i \in G \setminus G^{on}, \forall t \in [UT_i, \dots, |T|] \quad (4)$$

while the minimum down-time constraints are the following:

$$\sum_{\tau=t-DT_i+1}^t \delta_{i,\tau}^{off} \leq 1 - z_{i,t} \quad \forall i \in G \setminus G^{on}, \forall t \in [DT_i, \dots, |T|] \quad (5)$$

Given the initial on-off status of the unit  $z_i^{ini}$  (a parameter either equal to 0 or 1), the following inequalities are added to ensure that the unit completes the minimum up- or down-time in the current planning horizon if switched on or off in the previous one:

$$z_i^{ini} \leq z_{i,t} \quad \forall i \in G \setminus G^{on}, t = 1, \dots, \min(|T|, H_i^U) \quad (6)$$

$$z_i^{ini} \geq z_{i,t} \quad \forall i \in G \setminus G^{on}, t = 1, \dots, \min(|T|, H_i^D) \quad (7)$$

with  $H_i^U$  and  $H_i^D$  being the number of timesteps required to complete the minimum up- and down-time in the current horizon, respectively.

Finally, upward and downward ramping constraints are considered in the model:

$$p_{i,t} - p_{i,t-1} \leq RU_i z_{i,t-1} + SU_i \delta_{i,t}^{on} \quad \forall i \in G, \forall t = 2, \dots, |T| \quad (8)$$

$$p_{i,t-1} - p_{i,t} \leq RD_i z_{i,t} + SD_i \delta_{i,t}^{off} \quad (9)$$

where  $RU_i$  and  $RD_i$  are the unit's ramp-up and -down limits during nominal operation,  $SU_i$  and  $SD_i$  the ramping limits during start-up and shut-down. If the unit is already in operation at the beginning of the considered timestep (namely  $z_i^{ini} = 1$ ), then for  $t = 1$  the constraints take the following form:

$$p_{i,1} - p_i^{ini} \leq RU_i z_i^{ini} + SU_i \delta_{i,1}^{on} \quad \forall i \in G \quad (10)$$

$$p_i^{ini} - p_{i,1} \leq RD_i z_{i,1} + SD_i \delta_{i,1}^{off} \quad (11)$$

Please note that for those units that must run for all the time steps of the considered horizon (hence the ones belonging to the set  $G^{on}$ ), Eqs. (8)-(11) do not consider the terms  $SU_i \delta_{i,t}^{on}$  and  $SD_i \delta_{i,t}^{off}$ . In addition, the following constraints hold for ensuring that must-run units are in operation for the entire considered horizon, and the unavailable units are kept shut down at each time period:

$$z_{i,t} = 1 \quad \forall i \in G^{on}, \forall t \in T \quad (12)$$

$$z_{i,t} = 0 \quad \forall i \in G^{off}, \forall t \in T \quad (13)$$

### Reserve constraints

Reserve constraints are needed to ensure that whichever solution is evaluated, limited upwards and downwards fluctuation in the load demand at each node can be withstood. As a consequence, a sufficient number of generation units must make available part of their generation capacity for reserve purposes. This is enforced by defining variables related to the amount of generation power allocated as upward and downward reserve ( $r_{i,t}^{up}, r_{i,t}^{down}$ ) for each generation unit. At first, the generation reserve of each unit is limited by its maximum generation capacity and ramping capabilities:

$$0 \leq r_{i,t}^{up} \leq \min(\bar{P}_i - \underline{P}_i, RU_i) \cdot (1 - \delta_{i,t}^{on}) + (SU_i - \underline{P}_i) \delta_{i,t}^{on} \quad \forall i \in G, \forall t \in T \quad (14)$$

$$0 \leq r_{i,t}^{down} \leq \min(\bar{P}_i - \underline{P}_i, RD_i) \cdot (1 - \delta_{i,t+1}^{off}) + (SD_i - \underline{P}_i) \delta_{i,t+1}^{off} \quad (15)$$

Then, at each timestep the maximum reserve that can be provided is limited by the quantities committed to serve the demand:

$$r_{i,t}^{up} \leq z_{i,t} \bar{P}_i - p_{i,t} \quad \forall i \in G, \forall t \in T \quad (16)$$

$$r_{i,t}^{down} \leq p_{i,t} - z_{i,t} \underline{P}_i \quad (17)$$



Although Eqs. (14) and (15) consider the ramping capabilities of the unit, they do not capture the relationship between  $r_{i,t}^{up}$ ,  $r_{i,t}^{down}$  and the status of the unit among contiguous timesteps. For this reason, the following constraints are added:

$$r_{i,t}^{up} \leq RU_i z_{i,t-1} - (p_{i,t} - (p_{i,t-1} - r_{i,t-1}^{down})) + SU_i \delta_{i,t}^{on} \quad \forall i \in G, \quad (18)$$

$$r_{i,t}^{down} \leq RD_i z_{i,t} - (p_{i,t-1} + r_{i,t-1}^{up} - p_{i,t}) + SD_i \delta_{i,t}^{off} + (SD_i - \underline{P}_i) \delta_{i,t+1}^{off} \quad \forall t = 2, \dots, |T| \quad (19)$$

Starting from Eq. (18), it defines the upper bound of  $r_{i,t}^{up}$  depending on the operational condition. If the unit starts up at time  $t$ , then the upwards reserve is bounded by the ramping limit during startup  $SU_i$  (namely the available generation given by  $SU_i \delta_{i,t}^{on} - p_{i,t}$ ). On the other hand, if the unit was already running at  $t - 1$ , then the maximum quantity that can be offered as reserve is  $RU_i z_{i,t-1} - (p_{i,t} - (p_{i,t-1} - r_{i,t-1}^{down}))$ . The term  $p_{i,t-1} - r_{i,t-1}^{down}$  represents the power at the beginning of  $t$  (the downwards reserve is allocated to avoid any overestimate).

Regarding Eq. (19), the reserve  $r_{i,t}^{down}$  is dependent on the generation at the previous timestep and the downward ramping limit  $RD_i$ . If the unit is operating, the upper bound is defined by the term  $RD_i z_{i,t} - (p_{i,t-1} + r_{i,t-1}^{up} - p_{i,t})$ , with  $p_{i,t-1} + r_{i,t-1}^{up}$  the actual generation at the end of  $t - 1$  in case reserve is provided. In the timestep prior shutdown ( $\delta_{i,t+1}^{off} = 1$ ) the unit can ramp down from  $SD_i$  to  $\underline{P}_i$ , allowing a larger value than  $RD_i$  depending on the unit. Therefore the  $(SD_i - \underline{P}_i) \delta_{i,t+1}^{off}$  is added such that the binding constraints become Eq. (15) and (17). Finally, when the unit is shutdown the only non zeros are  $p_{i,t-1}$  and  $SD_i \delta_{i,t}^{off}$ , whose difference is always positive due to Eq. (9).

For the first timestep of the horizon, given the initial condition inherited from the previous horizon, the following constraints hold:

$$r_{i,1}^{up} \leq p_i^{ini} - p_{i,1} + RU_i z_i^{ini} + SU_i \delta_{i,1}^{on} \quad \forall i \in G \quad (20)$$

$$r_{i,1}^{down} \leq p_i^{ini} - p_{i,1} + RD_i z_{i,1} + SD_i \delta_{i,1}^{off} \quad (21)$$

Also here, must-run units share the same Eqs. (14)-(21), but the terms  $SU_i \delta_{i,t}^{on}$  and  $SU_i \delta_{i,t}^{off}$  are not present. Please note that in case the computational complexity allows to update the generators schedule frequently (e.g., every 10 minutes), and for applications where load fluctuation is limited, it is unlikely that most of the units are required to share their maximum upwards and downwards reserve quantities among contiguous time periods (and vice-versa). Therefore,  $r_{i,t-1}^{down}$  and  $r_{i,t-1}^{up}$  can be dropped from Eqs. (18) and (19), respectively (although resulting in a less conservative solution).

Finally, the following constraints are needed to ensure that the reserve requirements per each area of the network are met:

$$\sum_{i \in G_r} r_{i,t}^{up} \geq Res_{r,t}^{up} \quad \forall r \in R, \forall t \in T \quad (22)$$

$$\sum_{i \in G_r} r_{i,t}^{down} \geq Res_{r,t}^{down} \quad (23)$$

### System and security network constraints

Linearized system and security (N-1) constraints are considered in the MILP model in order to ensure feasible and reliable operation. These are needed to make sure that the generation and transmission schedule does not produce overload on any line both under nominal condition and in case the load is diverted because of a contingency in which at most one line fails.

Given  $x_{m,n}$ ,  $y_{m,n}$  and  $z_{m,n}$  the reactance, admittance and impedance of the line connecting bus  $m$  and  $n$ , the susceptance  $b_{m,n}$  can be evaluated. However, since the DC power flow model holds under the assumption of negligible line resistance with respect to its reactance [30],  $z_{m,n} \cong x_{m,n}$  and therefore  $b_{m,n} = -1/x_{m,n}$ . The Injection Shift Factors (ISFs) can be defined as follows [31]:

$$ISF_{m,n}^i = \frac{x_{m,i} - x_{n,i}}{x_{m,n}} \quad \begin{array}{l} m, n = y(c), \\ m, i = y(a), \\ n, i = y(e), \\ \forall c, a, e \in L, \\ \forall i \in B \end{array} \quad (24)$$

where  $y(c)$ ,  $y(a)$  and  $y(e)$  are the functions mapping the buses connecting lines  $c$ ,  $a$  and  $e$ .

These network sensitivity parameters represent the fraction of additional 1 MW injection at bus  $i$  that flows through the line connecting bus  $m$  and  $n$ . Once defined, the Power Transfer Distribution Factors (PTDFs) and Line Outage Distribution Factors (LODFs) according to [9] can be computed for each bus and line as follows:

$$PTDF_{m,n}^{i,j} = ISF_{m,n}^i - ISF_{m,n}^j \quad \begin{array}{l} m, n = y(c), \forall c \in L, \\ \forall i, j \in B \end{array} \quad (25)$$

$$LODF_{m,n}^{i,j} = \frac{PTDF_{m,n}^{i,j}}{1 - PTDF_{i,j}^{i,j}} \quad \begin{array}{l} m, n = y(c), \\ i, j = y(a), \\ \forall a, c \in L \end{array} \quad (26)$$

In particular,  $PTDF_{m,n}^{i,j}$  represents the variation of the power flowing on line  $c$  (connecting  $m$  and  $n$ ) resulting from the power transfer of 1 MW injected in bus  $i$  and consumed at bus  $j$ . On the other hand,  $LODF_{m,n}^{i,j}$  represents the fraction of pre-contingency power flowing from bus  $i$  to  $j$  (line  $a$ ) that is redistributed on the line connecting  $m$  and  $n$  (line  $c$ ) consequently the outage of the line linking  $i$  and  $j$  (line  $a$ ). Please note that  $ISF_{m,n}^i$  and  $LODF_{m,n}^{i,j}$  are the elements of the  $ISF$  and  $LODF$  matrices, which are needed for the definition of the following network constraints.

Under nominal operating conditions (no contingencies) the power flowing through each line must always be within the rated limits. This is imposed by the following constraint:

$$-\bar{F}_c \leq f_{c,t} \leq \bar{F}_c \quad \begin{array}{l} \forall c \in L \\ \forall t \in T \end{array} \quad (27)$$

where  $\bar{F}_c$  is the maximum allowed power flowing through line  $c$  in each direction ( $\bar{F}_c$  referred to flow limit going from bus  $m$  to  $n$ ,  $-\bar{F}_c$  for the one from  $n$  to  $m$ ). In particular, the power flow  $f_{c,t}$  is defined by the matrix  $ISF$ , the generated quantity  $p_{i,t}$  and total served demand ( $D_{b,t} - d_{b,t}^{shed}$ ) as follows:

$$f_{c,t} = \sum_{b \in B, i \in G_b^B, G_b^B \neq \emptyset} ISF_{m,n}^b \cdot \frac{p_{i,t}}{dt} - \sum_{b \in B} ISF_{m,n}^b \cdot \left( \frac{D_{b,t} - d_{b,t}^{shed}}{dt} \right) \quad \begin{array}{l} m, n = y(c), \\ \forall t \in T \end{array} \quad (28)$$

with  $\sum_{b \in B, i \in G_b^B, G_b^B \neq \emptyset} ISF_{m,n}^b \frac{p_{i,t}}{dt}$  the timestep average power flowing through line  $c$  due to the total power injected by the generators, and  $\sum_{b \in B} ISF_{m,n}^b \left( \frac{D_{b,t} - d_{b,t}^{shed}}{dt} \right)$  the timestep average power flowing on line  $c$  due to the total power consumption. Please note that since  $p_{i,t}$  and  $D_{b,t} - d_{b,t}^{shed}$  are expressed as energy,  $\frac{p_{i,t}}{dt}$  and  $\frac{D_{b,t} - d_{b,t}^{shed}}{dt}$  represent the average generation and consumption power within a given timestep.

Overload on any line must be avoided also under any contingency in which the outage of one line happens (N-1 contingency). At time  $t$ , the post-outage power  $f_{c,t}^d$  flowing through line  $c$  because of the outage of line  $d$  is defined as follows:

$$f_{c,t}^d = f_{c,t} + LODF_{m,n}^{j,k} \cdot f_{d,t} \quad \begin{array}{l} m, n = y(c), \\ j, k = y(d), \\ \forall t \in T \end{array} \quad (29)$$

where  $LODF_{m,n}^{j,k} \cdot f_{d,t}$  is the fraction of pre-outage power flowing through  $d$  that is diverted onto  $c$ . To find a solution where no post-contingency flow exceeds the line limits, the following N-1 security constraints are added:

$$-\bar{F}_c \leq f_{c,t}^d \leq \bar{F}_c \quad \begin{array}{l} \forall c, d \in L, \\ \forall t \in T \end{array} \quad (30)$$

In this way the solution is robust against any line outage.

The constraints described by Eq. (27) and (30) are the System and Security Network Constraints (SSNCs) of the problem.

### **Energy balance constraints**

At each timestep of the considered horizon the energy demand at each node must be met. This is enforced by the following equality:

$$\sum_{i \in G_b^B} p_{i,t} + \sum_{c \in L_b^{in}} f_{c,t} dt - \sum_{c \in L_b^{out}} f_{c,t} dt = D_{b,t} - d_{b,t}^{shed} \quad \forall b \in B, \forall t \in T \quad (31)$$

where  $\sum_{i \in G_b^B} p_{i,t}$  is the sum of the quantities generated by the units connected to bus  $b$ ,  $\sum_{c \in L_b^{in}} p_{c,t}^N$  and  $\sum_{c \in L_b^{out}} p_{c,t}^N$  the energy transmitted from bus  $b$  to other ones connected and vice versa,  $D_{b,t}$  and  $d_{b,t}^{shed}$  the requested and shed demand at bus  $b$  at time  $t$ .

For the linearized DC power flow model, the  $ISF$  matrix can be used to allocate the power flowing on each line of the network given the generation and consumption at each node. In addition, the presence of system and security network constraints (Eq. (27) and (30)) ensures that the generated power is routed on each line so as to avoid any overload under nominal and N-1 contingency conditions (therefore taking care of the balance at each node). Thus, Eq. (31) can be substituted by the following network balance:

$$\sum_{i \in G} p_{i,t} = \sum_{b \in B} (D_{b,t} - d_{b,t}^{shed}) \quad \forall t \in T \quad (32)$$

### **Objective function**

The objective function to minimize is the total operational cost over the specified time planning horizon, namely:

$$OF1 = \sum_{i \in G} \sum_{t \in T} (c_{i,t} p_{i,t} + c_i^{on} z_{i,t} + c_i^{su} \delta_{i,t}^{on} + c_i^{sd} \delta_{i,t}^{off}) + c^{shed} \sum_{b \in B} \sum_{t \in T} d_{b,t}^{shed} \quad (33)$$

where  $c_{i,t} p_{i,t}$  is the term related to the variable Operation and Maintenance (O&M) cost based on generation output,  $c_i^{on} z_{i,t}$  the term related to the fixed O&M hourly cost,  $c_i^{su} \delta_{i,t}^{on}$  the start-up cost,  $c_i^{sd} \delta_{i,t}^{off}$  the shut-down cost and  $c^{shed} d_{b,t}^{shed}$  the virtual cost linked to the amount of shed load ( $d_{b,t}^{shed} \in [0; D_{b,t}] \forall b \in B, \forall t \in T$ ). Note that in this case  $c^{shed}$  must be large enough in order to minimize the unmet demand. While  $OF1$  is considered as the reference objective function for this study, another objective function  $OF2$  is considered with the aim of assessing the impact on the computational time and solution:

$$OF2 = \sum_{i \in G} \sum_{t \in T} (c_{i,t} p_{i,t} + c_i^{on} z_{i,t} + c_i^{su} \delta_{i,t}^{on} + c_i^{sd} \delta_{i,t}^{off}) - \sum_{b \in B} \sum_{t \in T} c_{b,t}^d (D_{b,t} - d_{b,t}^{shed}) \quad (34)$$

Here the term  $c_{b,t}^d (D_{b,t} - d_{b,t}^{shed})$  represents the virtual revenue gained by serving the demand. By setting the parameter  $c_{b,t}^d$  large enough the optimal solution will maximize the amount of served demand at the minimum cost (similarly to maximizing the social welfare).

### 3.2. Solution approaches

The solution approaches considered in this work are four: one is taken from literature and used as benchmark while the other three contain elements of novelty. The first method (M1) is taken from literature and considered as reference [13]. It consists of an iterative approach that adds security constraints based on the violation of the current solution. The second method (M2) is a novel variation of M1 which includes additional features for the prediction of new violated constraints. The third one (M3) is a callback-based method, which integrates the features of M1 by means of solver callback functions. Finally, a novel shrinking horizon approach with non-uniform time discretization is presented as fourth solution approach (M4).

In all the proposed methods the initial optimization model does not consider any of the system and security network constraints, as these are added during the optimization algorithm. This is because considering all of them would make the model hard to solve, and most of the times only a small subset is needed (as previously mentioned in Section 1). However, the addition of network constraints ensures the feasibility of the optimal solution found. Finally, although all the proposed approaches do not consider any Umbrella Constraints Discovery algorithm (e.g., [32]), one can still be added for the sake of evaluating the starting set of system and contingency constraint.

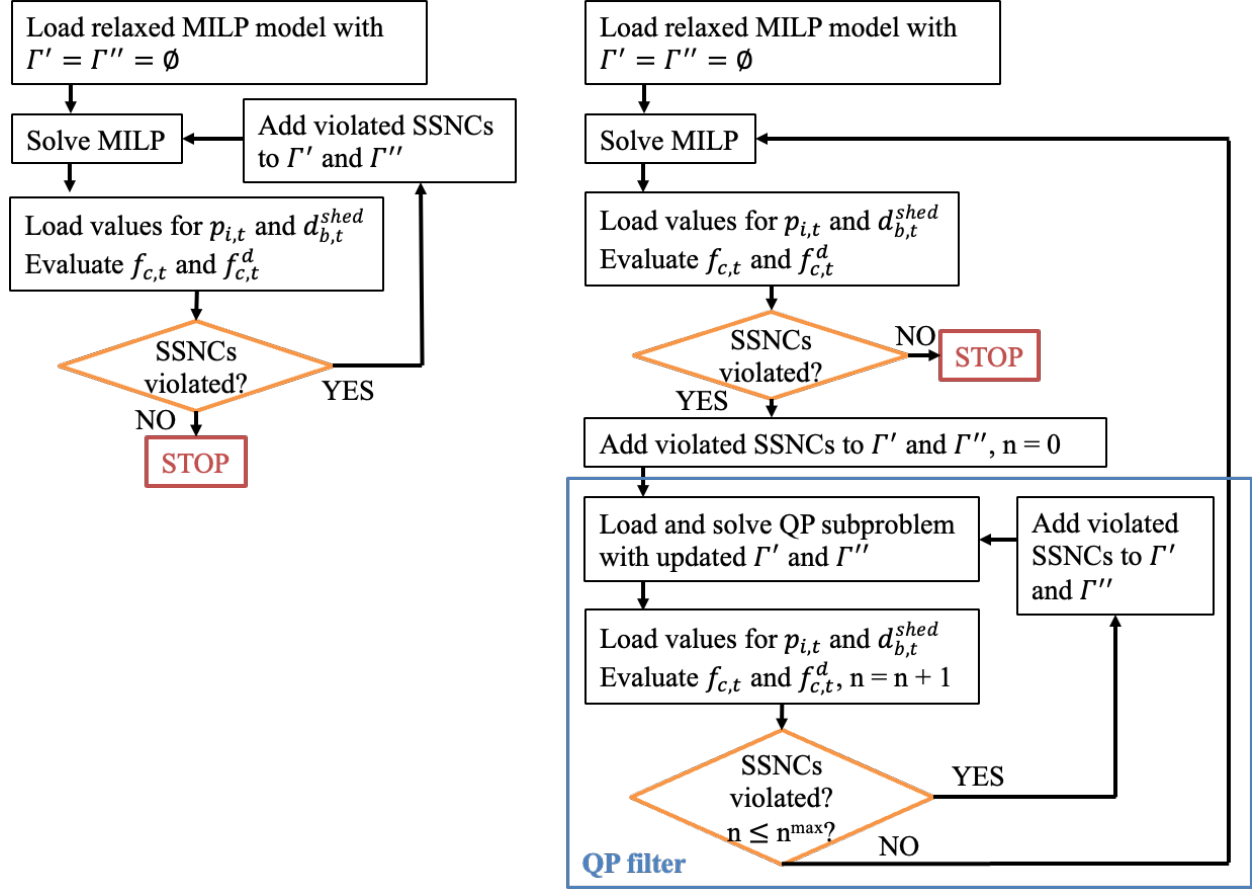


Figure 1 On the left: flowchart representing the solution approach M1. On the right: flowchart representing the solution approach M2. SSNCs are added to the sets of active constraints  $\Gamma'$  and  $\Gamma''$  based on how the current solution violate them.

### 3.2.1. Reference approach: iterative method based on constraint violation (M1)

The method considered as reference approach can be found in Xavier et al. [13] and the flowchart describing the algorithm can be seen in Figure 1 (left). This solution approach is based on an active-set strategy that aims at finding new system and security network constraints (SSNC) iteratively.

At first, a relaxed version of the SCUC model with no SSNCs is loaded (namely an MILP defined by Eqs. (1)-(23)). Then,  $\Gamma'$  and  $\Gamma''$  are defined as the sets containing the active SSNCs described by Eqs. (27) and (30) respectively. These two sets belong to the MILP model and are both empty at the first iteration (no active constraints have been discovered). Once a Unit Commitment solution is found, the pre- and post-contingency power flows ( $f_{c,t}$  and  $f_{c,t}^d$ ) are evaluated. Based on these, it is determined whether Eqs. (27) and (30) are met and they are ranked based on the degree of violation. The sets  $\Gamma'$  and  $\Gamma''$  (and thus the MILP model) are updated by adding the SSNCs with the highest violation on each line and time-step, as well as the other  $k$  ones with greatest infringement per each time-step (independently on the line). Please note that the authors suggested  $k$  between 5 and 15, depending on the network considered. In this study  $k$  was set equal to 15 for all cases for the sake of consistency (no sensitivity on this parameter was performed). The reason why not all violated constraints are added to the model at each iteration is because numerical results show how only a fraction of them are actually needed (as seen in [32] and [33]).

Finally, the algorithm stops when it finds an optimal solution that does not result in any violation of the SSNCs (hence the solution of the SCUC is found).

### 3.2.2. Iterative method based on QP filter (M2)

The approach presented here shares many of the features seen in the previous one, such as its iterative nature and the progressive addition of SSNCs. The main difference lies in the way these constraints are added to the SCUC model. While in the previous approach the SSNCs are selected just by the outcome of the “master” problem, here their evaluation depends also on the results of an operational subproblem modelled as a Quadratic Program (QP). Solving this model aims at finding the closest generation schedule to the one found in the relaxed SCUC while ensuring that the pre- and post-contingency power flows agrees with the SSNCs already in  $\Gamma'$  and  $\Gamma''$ . To achieve this, the subproblem is formulated as follows:

$$\min \sum_{i \in G, t \in T} (p_{i,t}^{QP} - \tilde{p}_{i,t})^2 \quad (35)$$

$$s. t. \quad \sum_{i \in G} p_{i,t}^{QP} = \sum_{b \in B} (D_{b,t} - \tilde{d}_{b,t}^{shed}) \quad \forall t \in T \quad (36)$$

$$0 \leq p_{i,t}^{QP} \leq \bar{P}_i \quad \forall i \in G, \forall t \in T \quad (37)$$

$$-\bar{F}_c \leq f_{c,t}^{QP} \leq \bar{F}_c \quad \forall c, t \in \Gamma' \quad (38)$$

$$-\bar{F}_c \leq f_{c,t}^{d,QP} \leq \bar{F}_c \quad \forall c, d, t \in \Gamma'' \quad (39)$$

with  $\tilde{p}_{i,t}$  and  $\tilde{d}_{b,t}^{shed}$  coming from the solution of the relaxed “master” SCUC problem at the current iteration and referred to the output of generation unit  $i$  at time  $t$  and the shed demand on bus  $b$  at time  $t$ , respectively. By minimizing the squared Euclidean distance in Eq. (35), the closest “new” generation schedule defined by  $p_{i,t}^{QP}$  is found. This solution features pre- and post-contingency flows  $f_{c,t}^{QP}$  and  $f_{c,t}^{d,QP}$  that meet all the active SSNCs (Eqs. (38) and (39)), as well as the network balance constraint (Eq. (36)).

The flowchart of the algorithm can be seen in Figure 1 (right). At first, the relaxed “master” problem is solved and SSNCs are added as for the M1 approach. Then, a further update of  $\Gamma'$  and  $\Gamma''$  is performed by repeatedly solving the QP subproblem (in this study 20 was considered given the preliminary computational outcomes). Per each time period, SSNCs are added based on their degree of infringement. As for M1, the algorithm is stopped once a solution that does not violate any SSNCs is found.

It is important to remark some aspects of the solution approach (M2), highlighting the difference with respect to M1. At first, the idea that motivates the proposed approach is presented. By considering M1, it finds new SSNCs to add based on the solution found at each iteration. Therefore, the newly added constraints are used to cut the current operational solution with the aim of finding another one that would hopefully satisfy all network requirements.

On the other hand, at each iteration the method M2 updates  $\Gamma'$  and  $\Gamma''$  based on the outcome of the (master) SCUC MILP problem (as for M1) and the results found by solving the QP subproblem for a limited number of times. In particular, every solution found by the QP problem represents the closest feasible ones to the master problem according to the updated set  $\Gamma'$  and  $\Gamma''$ . Therefore, the newly added SSNCs cut a larger set of SCUC solutions providing a prediction of potentially active constraints for the following iterations with the aim of limiting their number.

There are two main drawbacks with this approach. At first, in case the SSNCs violated by the master SCUC MILP are sufficient to find a new feasible integer solution that is substantially different than the previous one, the effort spent in solving multiple times the QP subproblem may not be worthwhile. Then, the solution found by the QP subproblem might be infeasible when applied to the SCUC model since the QP model does not include any of the operational constraints of the original one. That is why the QP model solved for a limited number of times: to avoid adding useless SSNCs linked to unfeasible solutions.

### 3.2.3. Solver callback-based method (M3)

The third method considered and developed in this paper considers the use of solver callback functions [34] for the discovery and addition of SSNCs. Similarly to refs. [22] and [35], network constraints are added during the branch-and-bound process as new integer solutions are found, without the need of repeatedly solving the model, thus aiming at saving the computational time. To do so, a callback function implementing part of the algorithm in M1 was developed. The reason why M1 was chosen over M2 is because the latter requires to solve an inner QP subproblem every time a solution is found. However, at the time of this work no commercially-available solver had this capability.

The way the callback works can be seen in Figure 1 (left). As for M1, a relaxed version of the SCUC model (MILP with constraints defined by Eqs. (1)-(23)) is considered with no SSNCs (empty sets  $\Gamma'$  and  $\Gamma''$  - see method M1). The model is loaded by the solver, and the Branch-and-Cut algorithm is started. Each time a new incumbent solution is found (new improved integer solution), the callback function is called by the solver. Thus, the numerical values of each variable of the incumbent solution are loaded, the pre- and post-contingency flow through each line is evaluated and the SSNCs are checked. The ones that are violated the most are added to  $\Gamma'$  and  $\Gamma''$  as for M1. Differently from the M1 and M2, constraints are added to the MILP as “Lazy Constraints” (which are constraints that are dynamically added during the optimization process based on the violation of the current solution, e.g., [36]), with the aim of reducing the computational burden.

A solution is found when the MIP gap is below the given limit and no SSNCs are violated.

### 3.2.4. Shrinking-horizon based method with solver callback (M4)

As previously mentioned, considering all SSNCs in the SCUC model makes it hard to solve, requiring a long computational time that is not in line with the requirements of most TSOs. Even if custom approaches are considered (as those presented in the previous sections), the total solution time could be longer than the desired one (e.g., 15-30 minutes). For this reason, a novel temporal decomposition approach inspired by the Shrinking Horizon algorithm (Balasubramanian and Grossmann [24]) and based on non-uniform time discretization is considered.

These two concepts are here described separately. At first, the Shrinking Horizon is a solution approach based on solving the same horizon in multiple runs. Starting from the first iteration, the original horizon is considered and a solution is found. Then, the solution belonging to the first  $\Delta t^{adv}$  periods (advancement periods) is stored, and a new horizon shrunk by those  $\Delta t^{adv}$  ones is considered for the next run. In addition, all variables not belonging to the  $\Delta t^{adv}$  timesteps can be relaxed to ease calculation.

Despite its ability to solve the “shrunk” problems faster (thanks to their reduced dimension), in the SCUC problem it is important to retain the integer nature of the variables due to the importance of time-linking constraints (e.g. duration constraints). Therefore, at the first iteration, the problem

will feature its full horizon (same complexity as the original problem). To solve this issue, non-uniform time discretization is introduced. The idea is to have a coarser time discretization for part of the horizon, reducing the number of timesteps and therefore the size of the problem (both variables and constraints). This approach is motivated by assuming that decisions at the beginning of the horizon are slightly influenced by the ones at the end of it. It is important to point out how the binary nature of some variables is kept in all timesteps (whether they are aggregated or not) such that the model does not degenerate (although some accuracy is lost).

In this work, the non-uniform discretization was implemented in the following way. At first, the original timestep discretization  $dt$  is considered and the values  $\Delta t^{adv}, \tilde{t} \in \mathbb{N}$  are defined. At each iteration, the time discretization of current horizon is modified. By considering  $T$  the number of timesteps of original duration  $dt$ , the first  $\Delta t^{adv}$  periods are kept as-is while the remaining  $T - \Delta t^{adv}$  are grouped into blocks of  $\tilde{t}$  timesteps. Of course,  $T - \Delta t^{adv}$  must be divisible by  $\tilde{t}$ , which must be a multiple of  $\Delta t^{adv}$ . Therefore, the horizon with uniform discretization  $dt$  goes from having  $T$  timesteps to  $\Delta t^{adv} + (T - \Delta t^{adv})/\tilde{t}$ , of which  $\Delta t^{adv}$  with discretization  $dt$  and  $T - \Delta t^{adv}$  with discretization  $\tilde{t}$ . This non-uniform discretization requires to modify the time series of the parameters by either summing or averaging (e.g., demand of  $\tilde{t}$  timesteps is summed, fuel cost if averaged).

Regarding the model, at each iteration the relaxed model with constraints defined by Eqs. (1)-(23) and no SSNCs is considered (as for the previous methods,  $\Gamma'$  and  $\Gamma''$  are empty). Given the new time discretization, ad-hoc time-linking constraints are developed with the aim of being consistent with the original formulation (e.g., time duration and ramping constraints) and keeping the integer nature of variables (the detailed description on how operational constraints were evaluated can be found in Appendix A SSCNs are added by means of the same callback function presented in method M3: This ensure that the solution found is feasible according to system and N-1 constraints. A schematic representation of the implemented decomposition can be seen in Figure 2, where the values used for the shrinking horizon advancement and modified discretization are used in this study ( $\Delta t^{adv} = 4, \tilde{t} = 4$  over an original time horizon of 24 one-hour timesteps).

At each run, the first  $\Delta t^{adv}$  original timesteps are kept, while the remaining ones are reorganized by means of aggregation in blocks of  $\tilde{t}$ . This results in a significant reduction in the number of considered timesteps (and thus problem size). For example, at the first iteration only nine timesteps are considered (against the 24 of the original problem). In addition, given these values of  $\Delta t^{adv}$  and  $\tilde{t}$ , only six iterations are needed to evaluate the 24-timestep solution.

Given the abovementioned description, it can be understood how combining a shrinking horizon approach with non-uniform time discretization can help finding a good solution in a reduced amount of time. Needless to say, two drawbacks are present: firstly, the solution found can be suboptimal; secondly, the problem reduction requires a careful model reformulation and parameter evaluation.



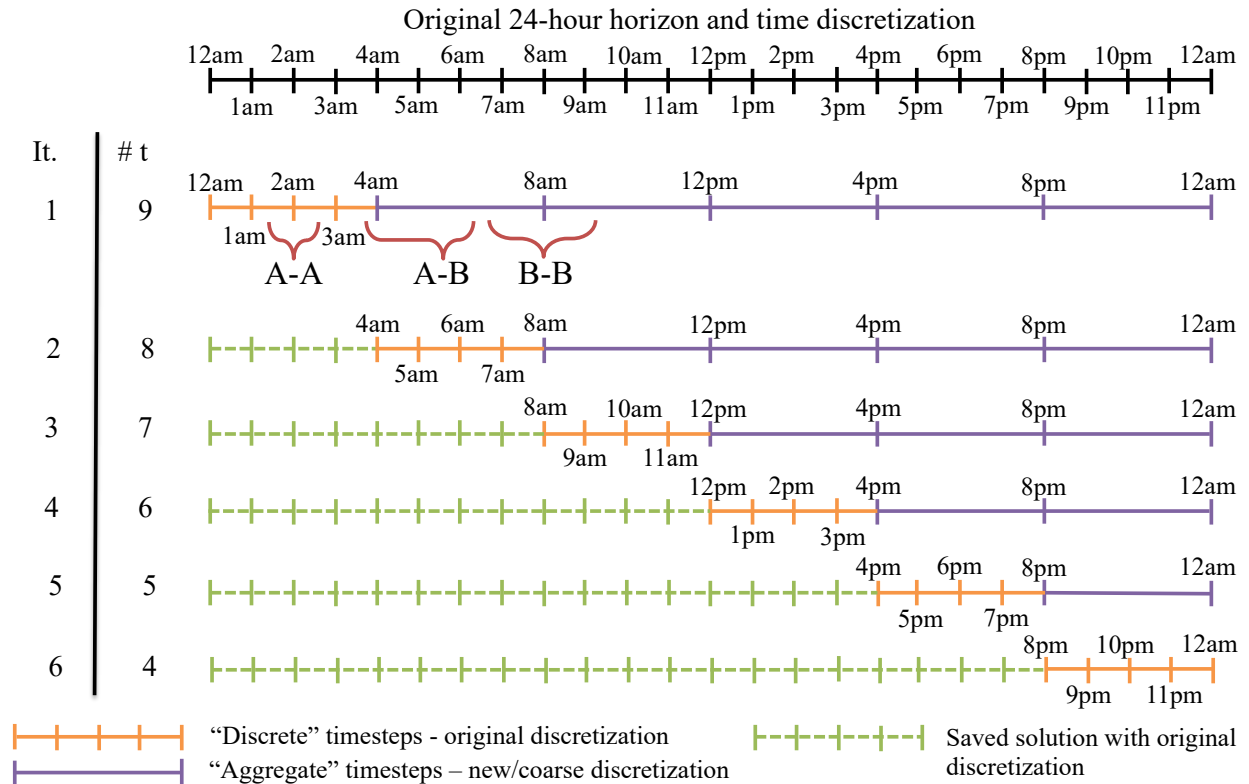


Figure 2 Schematic representation of the Shrinking Horizon algorithm presented in this study. The horizon considered in each iteration is the one comprising orange and purple timesteps: the former retain the same time discretization of the original time series within the considered horizon, while the latter consider a more coarse resolution (aggregating block of four intervals). The green dashed line represent the solution saved in the previous iteration.

## 4. Case studies

The different solution approaches presented in this work were tested and compared on five test cases. These are listed in Table 1 where the number on buses, generation units and lines are shown, as well as the number of variables and constraints of the original MILP model (before any per-solve operation) related to UC version of the problem (no SSNC). As previously mentioned, the solution approaches aim at reducing the computational time for the evaluation of an optimal and feasible SCUC solution. This is needed in case multiple, intra-day runs are executed during the day. As a consequence, the test cases consider random parameter profiles (e.g., demand at each node) generated from publicly available data. In addition, with the aim of simulating an intraday scheduling optimization, the 24-hour profiles may start from any hour of the day (e.g., from 4:00pm to 3:00pm of the day after).

Each test case was generated according to the methodology proposed in [37], that is based on the information provided by PGLIB [38] for the grid definition, and by PJM [39] for the bids, load data at each node and generator units parameters. Parameters include variable O&M and fuel costs, start-up and shutdown costs, minimum up- and down-time (hours), upwards and downwards ramping limits, minimum and maximum allowed load from year 2019.

The generated test cases (and the corresponding MILP models) have a time discretization of one hour. Therefore, each test instance is characterized by a 24-timestep time horizon.

All test were run on a workstation featuring a six-core Intel® i7 processor with 16 GB of RAM. The solver used was Gurobi 9.5 [40], with default settings except for the MIP gap that was set to 1% and the Time Limit to 8 hours for all cases except for “case6468rte”. This one, being the largest, was set to 30 hours.

Table 1 Case studies considered in this study and their most representative features.

Name	First hour of the horizon	Generators	Buses	Lines	System demand <ul style="list-style-type: none"> <li>• Max/Min [GW]</li> <li>• Average [GW]</li> <li>• Total (horizon) [GWh]</li> </ul>	Problem dimension (no SSNCs, no pre-solve) <ul style="list-style-type: none"> <li>• Continuous/Binary vars.</li> <li>• Constraints</li> </ul>
ieee118	13	17	118	186	<ul style="list-style-type: none"> <li>• 4.1/2.4</li> <li>• 3.3</li> <li>• 79.1</li> </ul>	<ul style="list-style-type: none"> <li>• 3697/1224</li> <li>• 2928</li> </ul>
wp2383	13	293	2383	2896	<ul style="list-style-type: none"> <li>• 14.0/11.98</li> <li>• 12.9</li> <li>• 309.1</li> </ul>	<ul style="list-style-type: none"> <li>• 64801/21096</li> <li>• 49296</li> </ul>
sp3120	18	452	3120	3693	<ul style="list-style-type: none"> <li>• 15.0/10.77</li> <li>• 13.46</li> <li>• 323.1</li> </ul>	<ul style="list-style-type: none"> <li>• 87289/32544</li> <li>• 76008</li> </ul>
pegase2869	24	487	2869	4582	<ul style="list-style-type: none"> <li>• 96.22/74.96</li> <li>• 86.94</li> <li>• 2086.48</li> </ul>	<ul style="list-style-type: none"> <li>• 66481/35064</li> <li>• 81888</li> </ul>
case6468rte	20	1295	6468	9000	<ul style="list-style-type: none"> <li>• 79.59/60.70</li> <li>• 71.93</li> <li>• 1726.41</li> </ul>	<ul style="list-style-type: none"> <li>• 164665/85032</li> <li>• 198480</li> </ul>

## 5. Results

In this section the results obtained on the selected test cases are shown for the four methodologies presented in this work: the reference iterative approach based on constraint violation (M1, section 3.2.1), the enhanced iterative approach based on M1 with a “Quadratic Programming” filter (M2, section 3.2.2), a call-back based method replicating the reference method M1 (M3, section 3.2.3), and a Shrinking Horizon algorithm with solver callback functions (M4, section 3.2.4). The computational time, together with the operational costs, cost of electricity, and percentage of served demand are shown with the aim of providing a comprehensive and exhaustive view.

Results are divided into two subsections: the first one showing the optimization outcomes when the objective function  $OF1$  (Eq. (33)) is considered in the model; the second related to  $OF2$  (Eq. (34)). In this way it is possible to assess the effects on the solution and computational requirements (e.g., time) related to considering the maximization of social welfare as objective function over the typical total operational costs. Please note that only the operational costs are presented so to have a fair comparison between the operational decisions. In this way the high cost of the shed demand in  $OF1$  and the revenues related to meeting the system demand in  $OF2$  are filtered out. Comparing

the plain results from considering the two objective functions would have been meaningless (i.e., given the same solution, the objective functions would be with opposite signs in most cases).

### 5.1. Model with objective function $OF1$

By considering Eq. (33) as the objective function, the model is the typical one found in SCUC problems where the energy balance constraint is relaxed by the addition of a shed demand penalty variable  $d_{b,t}^{shed}$ . The penalty cost  $c^{shed}$  was set to  $\$10^7$  to minimize the shed amount.

Starting from Figure 3, the total solution times for each approach are shown. Considering the two iterative approaches M1 and M2, a negligible solution time difference is seen for the smallest test case “ieee118”, while for the other ones M2 is significantly faster (between -58% and -74% reduction). The approach M1 was unable to find a solution for the case “sp3120” and the method timed out. When looking at the approach M3 (tackling the full model with callback function), the time required to get to the optimal solution is significantly decreased, especially for cases “sp3120” and “wp2383” (-33% and -66% with respect to M2), while a modest improvement was seen for “pegase2869”. This shows how implementing solver callback functions for embedding the evaluation of active network constraints in the branch and bound search is a promising option. When a solution approach based on the Shrinking Horizon is considered (method M4), a further reduction in computational time is achieved. This is very evident in the cases “sp3120” and “pegase2869”, where M4 was 15.5 and 55.4 times faster than M3, respectively.

It is important to point out that for the case “case6468rte” each solution method timed out (solver Time Out parameter for this case was set to 30 hours of CPU time). In fact, M1, M2 and M3 were not able to find a solution that did not violate any SSNCs within the given time, while M4 was not able to find a solution covering the entire horizon (time out before finishing all iterations). Similar comments can be made for case “sp3120” since M1 did not find a solution within the maximum allowed time.

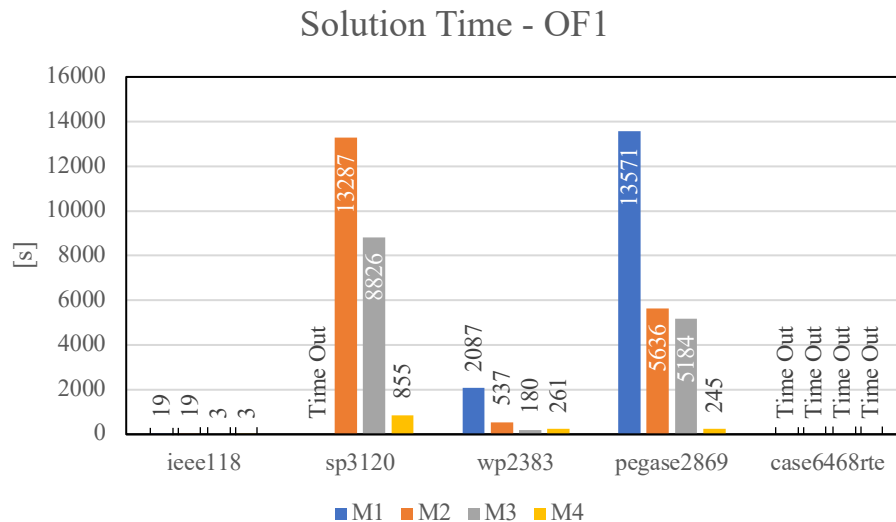


Figure 3 Solution time for the different method tested when model considers  $OF1$  as objective function.

An analysis on the impact of considering the QP subproblem in M2 with respect to the more traditional M1 approach can be seen in Table 2. This table shows the number of iterations needed

to obtain the optimal solution, as well as the total computational time spent for evaluating the SSNCs and how many of them are added. By looking at the numbers, it can be said that M2 requires fewer iterations, it spends more time in evaluating the SSNCs and it adds more of them in the model. The reason why M2 spends more time in evaluating SSNCs is because solving a QP subproblem for each timestep of the model takes significantly longer than just checking violated constraints and adding them to the set of active ones. At each iteration, M2 evaluates the security and network constraints violated by the current solution and the ones that are violated by the solutions of the QP subproblems. As a consequence, the number of added constraints per iteration is greater. This, however, reduces more the feasible region of the problem at each iteration and the SSNCs added by the QP subproblems prove to predict well the ones that would be added in the following iterations. This results in fewer iterations and an overall shorter solution time. Finally, it is important to note that the number of SSNCs added with M2 is almost 3 times greater than with M1, meaning that many of the added constraints are actually not needed for the optimal solution.

Table 2 Number of iterations, total time spent in evaluating the SSNCs and how many of them are added for each case using method M1 and M2 and considering objective function OF1 and OF2.

	<b>Iterations</b>			
	M1 (OF1)	M2 (OF1)	M1 (OF2)	M2 (OF2)
iecc118	16	6	14	4
sp3120	Time out	31	42	31
wp2383	11	8	11	7
pegase2869	45	11	46	11
case6468rte	Time out	Time out	48	10
<b>Time spent in SSNCs evaluation [s]</b>				
	M1 (OF1)	M2 (OF1)	M1 (OF2)	M2 (OF2)
iecc118	0.2	8.8	0.1	6.4
sp3120	Time out	1205.3	23.5	568.9
wp2383	4.0	60.2	4.3	46.6
pegase2869	17.3	311.9	16.1	160.7
case6468rte	Time out	Time out	72.9	1021.7
<b>Total SSNCs added</b>				
	M1 (OF1)	M2 (OF1)	M1 (OF2)	M2 (OF2)
iecc118	360	897	311	724
sp3120	Time out	2713	1014	2430
wp2383	244	630	232	532
pegase2869	1099	2001	1085	1686
case6468rte	Time out	Time out	1152	1612

The operational results are presented in Table 3, where the actual total operational cost over the considered horizon and the percentage of the total served demand are shown. At first it can be noticed how all cases that did not time out meet all the system demand. Just for one case this did not happen: the test case “pegase2869”. Here the solution obtained with the method M4 showed a 0.4% shed demand, corresponding to 6.47 GWh. The reason why this happens can be understood by looking at how the method M4 works and Figure 4. At the first iteration just the first four timesteps of the horizon retain the original parameters (discrete timesteps) while the other ones are aggregated. The optimal solution is the one that avoids any shed demand at the minimum operational cost both in the discrete and aggregate timesteps. Once the optimal solution for the first iteration is evaluated and the first four timesteps are saved, they are used to define the starting conditions for the subsequent shrunk horizon. However, these boundary conditions strongly reduce

the generator’s decision space, potentially making them unable to operate to serve the demand when the hourly (discrete) values are unveiled (due to the time-linking constraints related to ramping limits and minimum up/down time). This is what actually happens in case “pegase2869”, where the optimal decisions of Iteration 1 force the system to shed demand in the first four hours of Iteration 2 and 3.

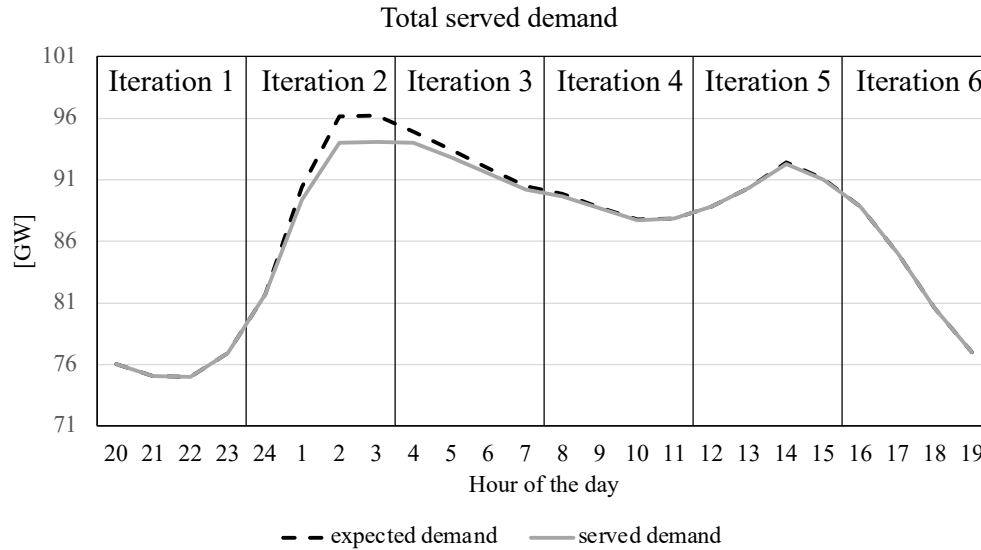


Figure 4 Solution obtained with the shrinking horizon approach M4 for pegase2869 at each iteration. Only the solution related to the first four discrete timestep is saved at each subsequent run.

Table 3 also shows the total operational cost of the different solutions found. By looking at the solutions obtained with the methods M1, M2 and M3 (which are exact methods), the difference is motivated by the chosen 1% MIP gap. When M4 is considered, instead, the optimal solution is achieved for cases “ieee118”, “sp3120” and “wp2383”, while a suboptimal solution is obtained for the other cases. In particular, the solution of “pegase2869” features a total operational cost +69% higher than the optimal one. Thus, not only the solution is not able to fully meet the demand, but its cost is also significantly higher. The reason why this happens is related to what was previously mentioned: as the horizon is shrunk and new, more precise discrete parameters are unveiled, the solution tries to adapt to minimize the shed demand, becoming suboptimal because of the previous decisions. Therefore, the commitments of Iteration 1 propagate to the next ones, shifting the decision process from finding the minimum operational cost to finding the solution that minimizes the shed demand.

Table 3 Operational results for each test case and solution method considered.

	Operational cost [k\$]							
	OF1				OF2			
	M1	M2	M3	M4	M1	M2	M3	M4
ieee118	2,486	2,406	2,413	2,423	2,243	2,223	2,255	2,230
sp3120	Time out	6,736	5,981	6,074	5,454	5,735	5,876	5,464
wp2383	3,332	3,361	3,415	3,344	3,386	3,800	3,395	3,324
pegase2869	21,957	21,999	21,914	37,041	18,279	18,346	18,514	20,186
case6468rte	Time out	Time out	Time out	Time out	11,616	11,763	12,717	11,654

	Demand served							
	OF1				OF2			
	M1	M2	M3	M4	M1	M2	M3	M4
ieee118	100%	100%	100%	100%	99.96%	99.95%	99.98%	99.97%
sp3120	Time out	100%	100%	100%	99.94%	99.95%	99.97%	99.08%
wp2383	100%	100%	100%	100%	99.98%	99.94%	100%	99.99%
pegase2869	100%	100%	100%	99.60%	99.98%	99.98%	100%	99.58%
case6468rte	Time out	Time out	Time out	Time out	99.67%	99.09%	99.62%	99.65%

	Cost of Electricity [\$/MWh]							
	OF1				OF2			
	M1	M2	M3	M4	M1	M2	M3	M4
ieee118	31.25	30.99	31.08	31.21	28.89	28.64	29.05	28.73
sp3120	Time out	18.75	18.58	18.87	16.95	17.83	18.26	17.13
wp2383	10.78	10.87	10.98	10.82	10.96	12.30	10.98	10.76
pegase2869	10.51	10.53	10.50	17.81	8.76	8.79	8.87	9.70
case6468rte	Time out	Time out	Time out	Time out	6.75	6.88	7.39	6.78

## 5.2. Model with objective function *OF2*

When Eq. (34) is considered as the objective function the solution will maximize the portion of the expected demand that maximizes the profit. This depends on the electricity price  $c_{b,t}^d$ , which must be set to a value higher than the generation cost. In this study  $c_{b,t}^d$  is time dependent and equal to the sum of the median and the 99<sup>th</sup> percentile of the system generation cost. Then, per each timestep the same value of  $c_{b,t}^d$  is shared across all buses. In this way the electricity prices are set to reasonable values simulating what happens in different regions of the world.

The results indicate that many things change with respect to the test cases considering *OF1*. At first, the total run time for the different test cases can be seen in Figure 5. Here it is evident how the computational time is greatly reduced with respect to the model featuring *OF1*. The overall reduction is between -11% and -93% when the same cases and methods are compared, and up to -99.2% when the fastest method with *OF2* is compared with the slowest with *OF1*. On the other hand, cases “ieee118” and “sp3120” showed an increase of +8.6% and +14.8% with M3, respectively.

While in the *OF1* cases a constant decrease in computational time was shown going from method M1 to M4, here this trend is not as evident. Considering the iterative methods M2 does not guarantee a clear computational advantage in all cases. Despite being significantly faster for case “pegase2869” (-60%) and “case6468rte” (-93%), similar solution times are seen in cases “ieee118” and “sp3120”. Regarding the case “ieee118”, being a small instance, the additional time spent in evaluating the SSNCs does not translate in an overall solution time reduction. For what concerns the case “sp3120”, the absence of run time reduction could be related to the solver logics, which are very hard to investigate.

Method M3 based on callback functions did not show any significant improvement over M2, resulting sometimes to be much slower. This is evident in cases “sp3120”, “pegase2869” and “case6468rte”. Finally, as for the previous cases where *OF1* was considered, M4 showed faster solution times across all test cases, with significant reductions.

When looking at Table 2, a comparison between the results obtained with M1 and M2 is shown. Here similar comments to the *OF1* can be made: M2 requires fewer iterations, it spends more time in evaluating SSNCs, and adds a greater number of them to the model. In general, by adopting *OF2*, a very similar number of iterations is required to obtain the optimal solution. On the other

hand, fewer SSNCs are added in both M1 and M2, despite the numbers remaining similar. The lower number of SSNCs also results into a reduction of the time spent in evaluating them.

### Solution time - OF2

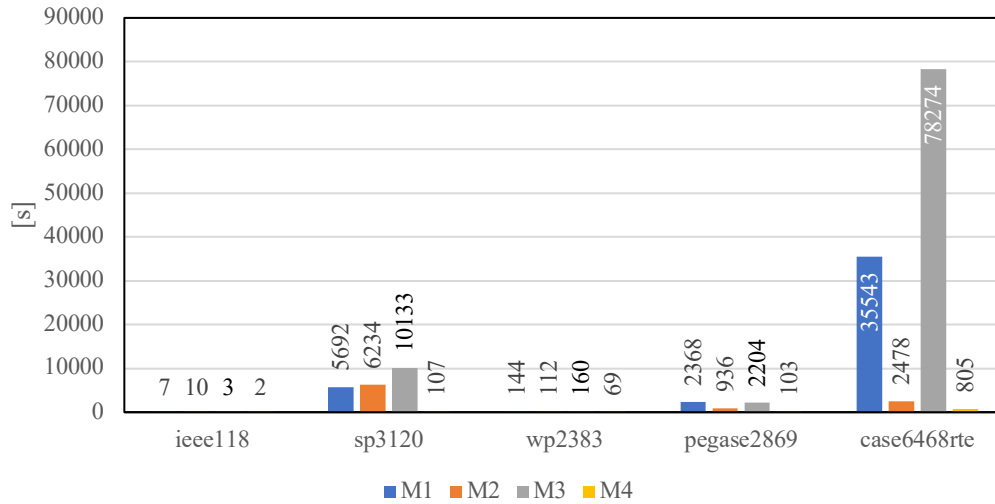


Figure 5 Solution time for the different method tested when model considers OF2 as objective function.

Finally, the operational results are presented in Table 3. The first thing that can be noted is how in almost all cases and methods the served demand is below 100%. However, the largest percentage of shed demand is 0.92% (“case6468r3”, M2), with an average value equal to 0.19%. Therefore, the amount of shed demand is very small. When the total operation costs are considered, they result to be lower than most cases evaluated with *OF1*, with a maximum reduction recorded of -45.5% (“pegase2869”, M4), and an average reduction across all cases of -11.8%. The reduction in operational cost also reflects in lower Costs of Electricity across most cases.

These results suggest that by changing the objective function of the model, better solutions can be found in a shorter time. The reason why different solutions are found can be understood by analyzing *OF1* and *OF2*. At first, given  $c_{b,t}^d$  large enough and a MIP gap set to 0%, solving the model with either *OF1* or *OF2* should bring the same solution, or at least solutions with the same operational cost. However, this does not occur due to three reasons. At first, solving the problem with *OF2* means that just the fraction of the demand that is most profitable is met, while considering not only the system constraints but also the N-1 contingency ones. As a consequence, it might happen that serving less demand is more profitable (thus justifying also lower operations cost). Then, given the high value of  $c^{shed}$  (set to  $10^7$ ) in *OF1*, numerical issues can occur, and thus affecting the final solution (e.g., a total shed demand of  $10^{-5}$  MWh across the whole horizon has a cost of 100 k\$). However, it is important to note that during the test phase, lower values of  $c^{shed}$  were considered and slower solution time were recorded (motivating therefore the choice). Finally, having set a MIP gap to 1% might results in finding different solutions as well. This is more evident when instead of analyzing the operational costs of the solutions, the expected profit is considered (which is what *OF2* evaluates). By looking at Table 4, it can be noted how the difference in profits between *OF1* and *OF2* are very limited. The largest differences are recorded when using method M4, which is expected since suboptimal decisions at the first iteration propagates across the other ones.



In conclusion, considering *OF2* resulted in a significant improvement in computational time, while showing very limited shed demand. Even for those cases where achieving zero shed demand is mandatory, the solution obtained with *OF2* can still be used as a warm start or for using heuristics. This could be particularly beneficial for cases where reducing the solution time is more important than guaranteeing optimality.

Table 4 Expected profits evaluated per each test case.

	Profits [k\$]							
	OF1				OF2			
	M1	M2	M3	M4	M1	M2	M3	M4
ieee118	300271	300192	300265	300230	300312 (+0.01%)	300304 (+0.04%)	300360 (+0.03%)	300363 (+0.04%)
sp3120	Time out	857294	857574	857452	857418 (n.c.*)	857616 (+0.04%)	857456 (-0.01%)	850158 (-0.85%)
wp2383	1821952	1821981	1821898	1821945	1820466 (-0.08%)	1821505 (-0.03%)	1821916 (+0.00%)	1821742 (-0.01%)
pegase2869	10705909	10705867	10705952	10647914	10707099 (+0.01%)	10707125 (+0.01%)	10706864 (+0.01%)	10660145 (+0.11%)
case6468rte	Time out	Time out	Time out	Time out	8833581 (n.c.*)	8781962 (n.c.*)	8828043 (n.c.*)	8831768 (n.c.*)

\*: non computable since timed out and no feasible solution was found.

## 6. Conclusions

This work presents three novel solution approaches for the SCUC problem. The solution approaches were tested over 5 test cases with two different objective functions and compared with a well-known iterative approach in literature.

When total operational cost (*OF1*) is considered as objective function, the comparison between the methods M1-M4 shows how the fastest is the one based on the Shrinking Horizon approach (M4), followed by M3 and M2. For the test cases considered, a reduction in computational time with respect to M1 of up to -74.2%, -91.36% and -98.19% was recorded for M2, M3 and M4 respectively. Regarding the solutions found, all methods presented similar solution with the only exception of M4 for case “pegase2869” (here 0.4% shed demand was present).

When considering *OF2* as objective function of the model, that includes virtual revenues for serving the demand, the first thing that can be noted is how the computational time is significantly reduced. By comparing each solution approach, the reduction in time is up to -93%, -83.4%, -57.5% and -87.44% for M1, M2, M3 and M4 respectively. Overall, M4 is still the fastest. Finally, it is important to point out that the solutions obtained with *OF2* are slightly different from the ones found with *OF1*, since they aim at maximizing the overall profit (up to +0.11% higher than *OF1*) at the cost of shedding part of the demand (up to 1%).

In conclusion, this paper has proved how the use of a Shrinking Horizon approach together with the solver callback functions to significantly reduce the computational time while finding good quality solutions. In addition, by investigating the use of different objective functions, it was shown how similar solution can be found for a fraction of the time. Future work should focus on improving the computational efficiency of callback functions on different solvers, finding better approaches to predict SSNCs, and evaluate the impact of using the solution found with *OF2* as a warm start of the problem with *OF1*.



## Appendix A

In this section the modelling of the operational constraints valid for the “aggregate” timesteps introduced with method M4 are presented.

### **Modelling of generation bounds, energy balance, system and security network constraints, and objective function.**

At each timestep, the amount of electrical energy that the generators can produce is limited by the upper and lower bounds. Since the parameters  $\underline{P}_i$  and  $\bar{P}_i$  are related to the minimum and maximum generation allowed for the original time step duration  $dt$  (one hour in this work), Eq. (1) holds  $\forall t \in T^{disc}$ . On the other hand, when dealing with aggregated timesteps, the constraint translates to the following:

$$\underline{P}_i z_{i,t} \leq p_{i,t} \leq (\tilde{t} \cdot \bar{P}_i) z_{i,t} \quad \forall i \in G, \forall t \in T^{agg} \quad (\text{A.1})$$

with  $\tilde{t}$  being the number of original timesteps with length  $dt$  contained in an aggregate one. The reason  $\underline{P}_i$  is the lower bound in the aggregate timesteps is because the units could be switched on only for some of the  $\tilde{t}$  aggregated timesteps.

Regarding the energy balance, Eq. (32) holds  $\forall t \in T^{disc}$ . For the aggregate timesteps, the constraint becomes:

$$\sum_{i \in G} p_{i,t} = \sum_{b \in B} (D_{b,t}^{agg} - d_{b,t}^{shed}) \quad \forall t \in T^{agg} \quad (\text{A.2})$$

where  $D_{b,t}^{agg}$  is the sum of the demand of the  $\tilde{t}$  timesteps belonging to the aggregate one.

The SSNCs described by the Eq. (27), (29) and (30) do not change for any of the discrete and aggregate timestep. What changes is the definition of the power flowing through line  $c$ :

$$f_{c,t} = \sum_{b \in B, i \in G_b^B, G_b^B \neq \emptyset} ISF_{m,n}^b \cdot \frac{p_{i,t}}{\tilde{t} \cdot dt} - \sum_{b \in B} ISF_{m,n}^b \cdot \left( \frac{D_{b,t}^{agg} - d_{b,t}^{shed}}{\tilde{t} \cdot dt} \right) \quad \begin{matrix} m, n = y(c), \\ \forall t \in T^{agg} \end{matrix} \quad (\text{A.3})$$

In this way, for  $t \in T^{agg}$  the term  $f_{c,t}$  refers to the average power flow in the aggregate timestep. The objective function keeps being either Eq. (33) and (34). The only difference is that any time-dependent cost parameters will have to be modified such that it is referred to a discrete or aggregate timestep. In particular, cost parameters related to aggregate timesteps are evaluated as the average of the elements belonging to them.

### **Modelling of ramping constraints.**

Time linking constraints considered in the model are the ones related to the ramping limits (Eq. (8) and (9)), minimum up- and down-time (Eqs. (2)-(7)) and reserve (Eqs. (14)-(23)).

Starting from the ramping limits, they represent the maximum increase and decrease of units' generation between adjacent timesteps. By looking at Figure 2, three different couples of adjacent timesteps can be identified: A-A, A-B and B-B. A-A refers to a couple of discrete timesteps, A-B to a couple where an aggregate timestep follows a discrete one, and B-B to a couple of aggregate timesteps. Since the aggregate and discrete timestep are characterized by different timestep duration, also the maximum allowed increase/decrease in generation among adjacent time intervals will change.

The general formulation of the constraints considered for the general couple of adjacent timesteps X and Y is the following:

$$p_{i,t} - p_{i,t-1} \leq RU_i^{X-Y} z_{i,t-1} + SU_i^{X-Y} \delta_{i,t}^{on} \quad \forall i \in G \quad (\text{A.4})$$

$$p_{i,t-1} - p_{i,t} \leq RD_i^{X-Y} z_{i,t} + SD_i^{X-Y} \delta_{i,t}^{off} \quad \forall t = T^* \quad (\text{A.5})$$

$$t \in T^{**}, t-1 \in T^{***}$$

The values related to the parameters  $RU_i^{X-Y}$ ,  $RD_i^{X-Y}$ ,  $SU_i^{X-Y}$ ,  $SD_i^{X-Y}$  and the sets  $T^*$ ,  $T^{**}$  and  $T^{***}$  can be found in Table A.1 Table A.1 per each case.

Table A.1 How parameters and sets in Eq. (A.4) and (A.5) are defined depending on the timestep couples considered in the reduced MILP with aggregate timesteps.

	A-A	A-B	B-B
$RU_i^{X-Y}$	$RU_i$	Eq. (A.10)	Eq. (A.11) <b>Error!</b> <b>Reference source not found.</b>
$RD_i^{X-Y}$	$RD_i$	Eq. (A.16)	Eq. (A.17)
$SU_i^{X-Y}$	$SU_i$	Eq. (A.19)	
$SD_i^{X-Y}$	$SD_i$	Eq. (A.21)	Eq. (A.22)
$T^*$	$\forall t = 2, \dots,  T^{disc} $	$\{ \min(t) \in T^{agg} \}$	$t: t > \min(t) \in T^{agg}$
$T^{**}$	$T^{disc}$	$T^{agg}$	$T^{agg}$
$T^{***}$	$T^{disc}$	$T^{disc}$	$T^{agg}$

It is now presented how the different parameters are evaluated for each timestep couple in the model.

The operational *ramp-up* limit is computed as the difference between the maximum generation achievable in an aggregate timestep starting from the minimum allowed generation in the previous timestep. Given  $RU_i$  the maximum allowed generation increase between adjacent timesteps for unit  $i$ , the minimum number of discrete timesteps needed to augment the unit's output from minimum to maximum is defined as follows:

$$\#RU_i = \left\lfloor \frac{\bar{P}_i - \underline{P}_i}{RU_i} \right\rfloor \quad (\text{A.6})$$

The reason why  $\#RU_i$  is evaluated as the floor of  $(\bar{P}_i - \underline{P}_i)/RU_i$  can be seen in Figure A.1 **Error! Reference source not found.** (dashed red line above the maximum generation line). Given, for example,  $(\bar{P}_i - \underline{P}_i)/RU_i = 2.6$  and the discrete nature of the timesteps, the decimal part must be truncated. By rounding up,  $\#RU_i$  would be equal to 3, therefore resulting higher than the maximum allowed. On the contrary, by rounding down,  $\#RU_i$  is equal to 2 (within the bounds) and the remaining part of the ramp corresponds to a load variation of  $0.6 \cdot RU_i$ , which can be allocated in the following timestep.

To evaluate the upward ramping limit either between a discrete and aggregate timesteps or two aggregate timesteps, it is necessary to calculate the difference among the minimum allowed generation in the previous interval and the maximum that can be achieved. For a A-B couple, the energy generated by the unit  $i$  in the previous discrete timestep is equal to the minimum load:

$$p_{t-1}^A = \underline{P}_i \quad (\text{A.7})$$

On the other hand, the unit's output for the previous aggregate timestep (thus related to the timestep couple B-B) is:

$$p_{t-1}^B = \tilde{t} \cdot P_i \quad (\text{A.8})$$

The maximum generation achievable in one aggregate timestep starting from the minimum load condition is defined by the following expression (a graphical representation of  $p_t$  can be seen in Figure A.1):

$$p_t^B = \underline{P}_i \min(\tilde{t}, \#RU_i) + \bar{P}_i \max(0, \tilde{t} - \#RU_i) + \sum_{n=1}^{\max(\tilde{t}, \#RU_i)} n \cdot RU_i \quad (\text{A.9})$$

Therefore, the  $RU_i^{A-B}$  and  $RU_i^{B-B}$  can be evaluated as follows:

$$RU_i^{A-B} = \underline{P}_i (\min(\tilde{t}, \#RU_i) - 1) + \bar{P}_i \max(0, \tilde{t} - \#RU_i) + \sum_{n=1}^{\min(\tilde{t}, \#RU_i)} n \cdot RU_i \quad (\text{A.10})$$

$$RU_i^{B-B} = \underline{P}_i (\min(\tilde{t}, \#RU_i) - \tilde{t}) + \bar{P}_i \max(0, \tilde{t} - \#RU_i) + \sum_{n=1}^{\min(\tilde{t}, \#RU_i)} n \cdot RU_i \quad (\text{A.11})$$

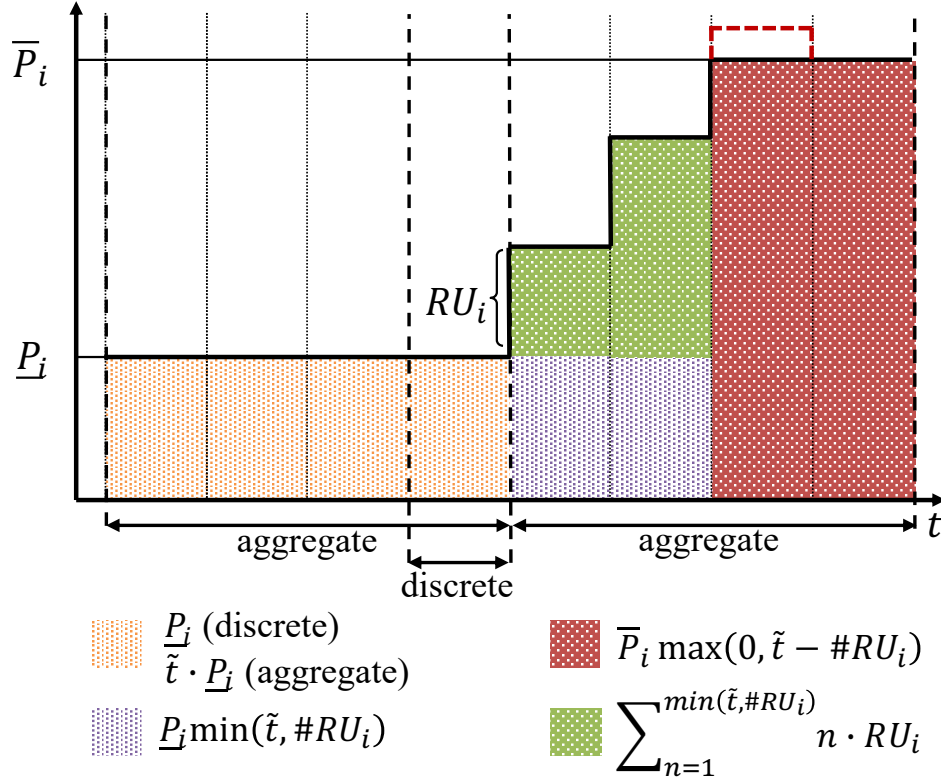


Figure A.1 Schematic representation of the maximum allowed generation increase between adjacent timesteps (A-B and B-B couples).

In a similar fashion, for the timestep couples A-B and B-B the *ramp-down* limit is evaluated as the difference between the generation related to ramping from maximum to minimum load, and the minimum allowed generation in the subsequent timestep. Given  $RD_i$  the maximum allowed

generation decrease between subsequent timesteps for unit  $i$ , the minimum number of discrete timesteps needed to reduce the unit's output from maximum to minimum is defined as follows:

$$\#RD_i = \left\lfloor \frac{\bar{P}_i - \underline{P}_i}{RD_i} \right\rfloor \quad (\text{A.12})$$

Rounding down  $(\bar{P}_i - \underline{P}_i)/RD_i$  is motivated by the same reason presented for upwards ramping limits case and can be seen in Figure A.2 (red dashed line): in case  $\#RD_i$  would be rounded up, the resulting generation at the end of the ramp would be lower than  $\underline{P}_i$ .

The maximum allowed generation for the discrete timestep (related to the timestep couple A-B) is equal to the maximum load:

$$p_{t-1}^A = \bar{P}_i \quad (\text{A.13})$$

On the other hand, the unit's output for the previous aggregate timestep (thus related to the timestep couple A-B) is:

$$p_{t-1}^B = \tilde{t} \cdot \bar{P}_i \quad (\text{A.14})$$

The minimum generation achievable in one aggregate timestep starting from the maximum load condition is defined by the following expression (a graphical representation of  $p_t$  can be seen in Figure A.2):

$$p_t^B = \underline{P}_i \max(0, \tilde{t} - \#RD_i) + \sum_{n=1}^{\min(\tilde{t}, \#RD_i)} (\bar{P}_i - n \cdot RD_i) \quad (\text{A.15})$$

Therefore, the  $RD_i^{A-B}$  and  $RD_i^{B-B}$  can be evaluated as follows:

$$RD_i^{A-B} = \bar{P}_i (1 - \min(\tilde{t}, \#RD_i)) - \underline{P}_i \max(0, \tilde{t} - \#RD_i) + \sum_{n=1}^{\min(\tilde{t}, \#RD_i)} n \cdot RD_i \quad (\text{A.16})$$

$$RD_i^{B-B} = \bar{P}_i (\tilde{t} - \min(\tilde{t}, \#RD_i)) - \underline{P}_i \max(0, \tilde{t} - \#RD_i) + \sum_{n=1}^{\min(\tilde{t}, \#RD_i)} n \cdot RD_i \quad (\text{A.17})$$

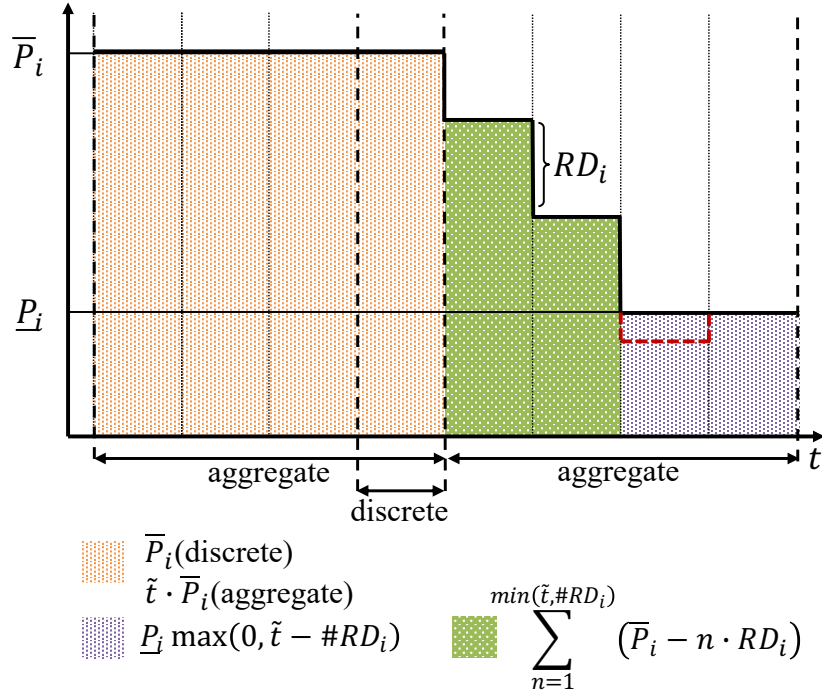


Figure A.2 Schematic representation of the maximum allowed generation decrease between adjacent timesteps (A-B and B-B couples).

Regarding the ramping limits related to *start-up* and *shut down*, they are equal to the maximum generation achievable before starting up and shutting down respectively.

Given  $SU_i$  the maximum allowed generation during the time-step of duration  $dt$  when the unit  $i$  switches on, the following term defines the minimum number of timesteps required to increase the output from  $SU_i$  to its maximum value.

$$\#SU_i = \left\lfloor \frac{\bar{P}_i - SU_i}{RU_i} \right\rfloor \quad (\text{A.18})$$

The value comes from rounding down  $(\bar{P}_i - SU_i)/RU_i$  for the same reasons seen above. Whatever the timestep prior the start-up is discrete or aggregate, the unit's output is null. Therefore  $p_{t-1}^A = p_{t-1}^B = 0$ . The maximum output achievable in one aggregate timestep at start up is limited by  $RU_i$ . It follows this expression, which also defines  $SU_i^{A-B}$  and  $SU_i^{B-B}$ :

$$\begin{aligned}
 SU_i^{A-B} &= SU_i^{B-B} = \\
 &= SU_i [1 + \min(\tilde{t} - 1, \#SU_i)] + \sum_{n=1}^{\min(\tilde{t}-1, \#SU_i)} n \cdot RU_i + \bar{P}_i [\tilde{t} - \min(\tilde{t} - 1, \#SU_i) - 1] \quad (\text{A.19})
 \end{aligned}$$

The abovementioned equation is graphically represented in Figure A.3.

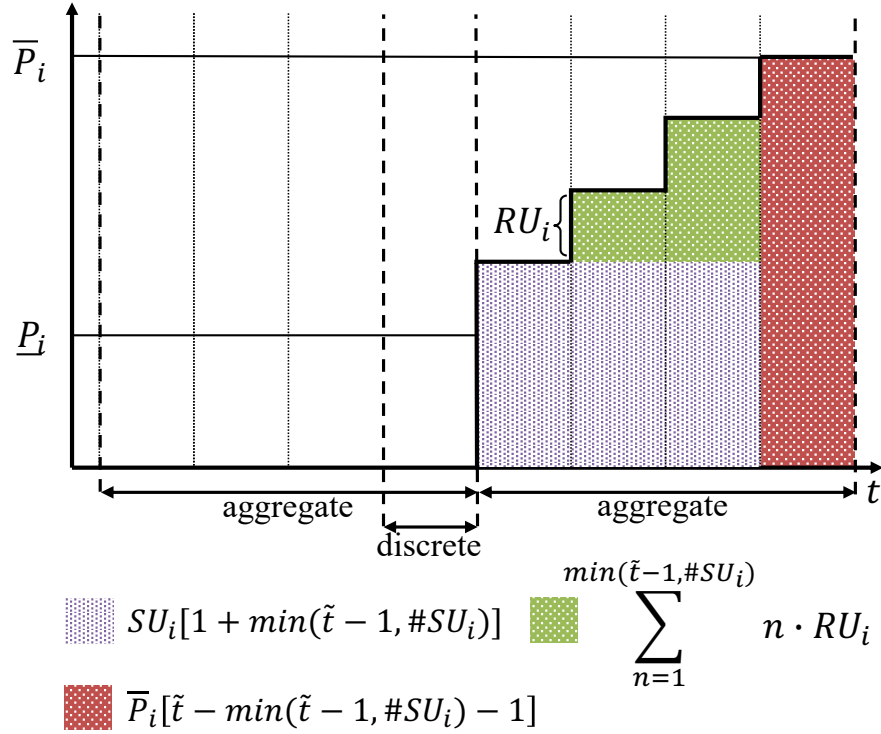


Figure A.3 Schematic representation of the maximum allowed generation at start up (A-B and B-B couples).

As for the start-up, also the ramping limit prior a shutdown is evaluated as the maximum allowed generation before turning the unit off. Given  $SD_i$  the maximum allowed generation in the timestep of duration  $dt$  prior shutdown, the following term defines the minimum number of timesteps required to decrease the output from its maximum value to  $SD_i$ .

$$\#SD_i = \left\lfloor \frac{\bar{P}_i - SD_i}{RD_i} \right\rfloor \quad (\text{A.20})$$

The value comes from rounding down  $(\bar{P}_i - SD_i)/RD_i$  for the same reasons seen in the subsections above. Whatever the timestep is discrete or aggregate, the unit's output is null if shutdown. Therefore  $p_t^B = 0$ . The maximum output allowed in one discrete timestep prior shutdown is the following:

$$SD_i^{A-B} = p_{t-1}^A = SD_i \quad (\text{A.21})$$

When an aggregate timestep is considered, then the following expression holds:

$$SD_i^{B-B} = SD_i + \bar{P}_i[\tilde{t} - \min(\tilde{t} - 1, \#SD_i) - 1] + \sum_{n=1}^{\min(\tilde{t}-1, \#SD_i)} (\bar{P}_i - n \cdot RD_i) \quad (\text{A.22})$$

The above-mentioned equation is graphically represented in Figure A.4.

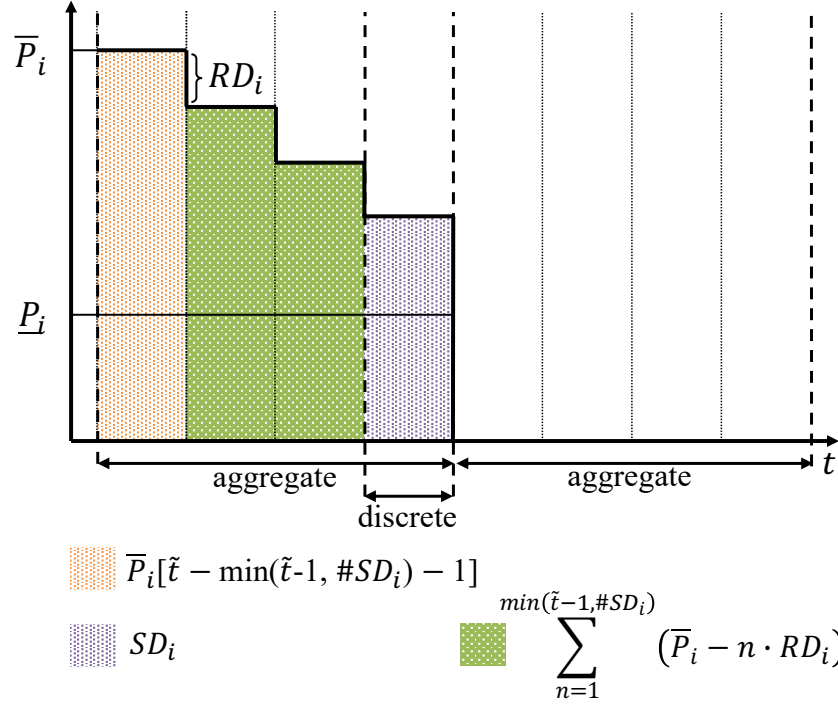


Figure A.4 Schematic representation of the maximum allowed generation before shut down (A-B and B-B couples).

### Modelling of minimum up- and down-time constraints.

The minimum up- and down-time constraints considered are the ones described by Eq. (4) and (5). As for the ramping limits, the parameters related to these constraints must be evaluated again in light of the presence of aggregate timesteps in the reduced problem. In fact,  $UT_i$  and  $DT_i$  are related to discrete timesteps with original length of  $dt$ . Four new parameters are introduced:  $\widetilde{UT}_{i,t}$ ,  $\widetilde{DT}_{i,t}$ ,  $\widetilde{UT}_i^{agg}$  and  $\widetilde{DT}_i^{agg}$ . They take part of constraints as follows:

$$\sum_{\tau=t-\widetilde{UT}_{i,t}+1}^t \delta_{i,\tau}^{on} \leq z_{i,t} \quad \forall i \in G \setminus G^{on}, \forall t \in [\widetilde{UT}_i^{agg}, \dots, |T|] \quad (A.23)$$

$$\sum_{\tau=t-\widetilde{DT}_{i,t}+1}^t \delta_{i,\tau}^{off} \leq 1 - z_{i,t} \quad \forall i \in G \setminus G^{on}, \forall t \in [\widetilde{DT}_i^{agg}, \dots, |T|] \quad (A.24)$$

with  $T = T^{disc} \cup T^{agg}$ . The parameters  $\widetilde{UT}_{i,t}$  and  $\widetilde{DT}_{i,t}$  are defined for only  $t \geq \widetilde{UT}_i^{agg}$  and  $t \geq \widetilde{DT}_i^{agg}$  respectively.

At first,  $\widetilde{UT}_i^{agg}$  and  $\widetilde{DT}_i^{agg}$  are defined as the minimum number of discrete and aggregate timesteps corresponding to the original  $UT_i$  and  $DT_i$ . As a consequence, if  $UT_i \leq \Delta t^{adv}$  and  $DT_i \leq \Delta t^{adv}$ , then  $\widetilde{UT}_i^{agg} = UT_i$  and  $\widetilde{DT}_i^{agg} = DT_i$ . On the other hand, if  $UT_i > \Delta t^{adv}$  and  $DT_i > \Delta t^{adv}$  then the following expressions hold:

$$\widetilde{UT}_i^{agg} = \Delta t^{adv} + \left\lceil \frac{UT_i - \Delta t^{adv}}{\tilde{t}} \right\rceil \quad (A.25)$$

$$\widetilde{DT}_i^{agg} = \Delta t^{adv} + \left\lceil \frac{DT_i - \Delta t^{adv}}{\tilde{t}} \right\rceil \quad (\text{A.26})$$

The parameter  $\widetilde{UT}_{i,t}$  is not defined for  $t < \widetilde{UT}_i^{agg}$ ,  $\widetilde{UT}_{i,t} = \widetilde{UT}_i^{agg}$  for  $t = \widetilde{UT}_i^{agg}$ , while the following expression holds for  $t > \widetilde{UT}_i^{agg}$ :

$$\begin{aligned} \widetilde{UT}_{i,t} = & \max \left( 0, UT_i - \max \left( 0, \min(t - \Delta t^{adv}, \left\lceil \frac{UT_i}{\tilde{t}} \right\rceil \right) \right) \right) \cdot \tilde{t} \\ & + \max \left( 0, \min(t - \Delta t^{adv}, \left\lceil \frac{UT_i}{\tilde{t}} \right\rceil \right) \end{aligned} \quad (\text{A.27})$$

The same applies for  $\widetilde{DT}_{i,t}$ : it is not defined for  $t < \widetilde{DT}_i^{agg}$ ,  $\widetilde{DT}_{i,t} = \widetilde{DT}_i^{agg}$  for  $t = \widetilde{DT}_i^{agg}$ , and the following expression holds for  $t > \widetilde{DT}_i^{agg}$ :

$$\begin{aligned} \widetilde{DT}_{i,t} = & \max \left( 0, DT_i - \max \left( 0, \min(t - \Delta t^{adv}, \left\lceil \frac{DT_i}{\tilde{t}} \right\rceil \right) \right) \right) \cdot \tilde{t} \\ & + \max \left( 0, \min(t - \Delta t^{adv}, \left\lceil \frac{DT_i}{\tilde{t}} \right\rceil \right) \end{aligned} \quad (\text{A.28})$$

The reason why the Eq. (A.25) and (A.26) rounds up the value in the ratio is to ensure that the minimum up- and down-time are respected (this might not happen if rounding down). However, this comes at the cost that decisions could potentially be suboptimal. An example of how the constraints are modelled can be seen in Figure A.5.

$$UT_i = 10, \quad \widetilde{UT}_i^{agg} = 6, \quad \widetilde{UT}_{i,t} = [-, -, -, -, -, 6, 3, 3, 3]$$

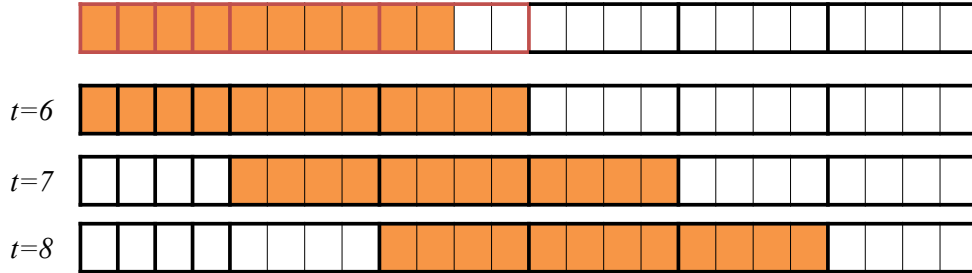


Figure A.5 Schematic representation of how the minimum up-time constraints are modelled in the reduced MILP with aggregate timesteps.

### Modelling of reserve constraints.

The constraints defined by Eqs. (14)-(17), and (22) and (23) remain the same in the reduced problem, with the exception that the parameters are multiplied by  $\tilde{t}$  for those timesteps belonging to  $T^{agg}$ .

On the other hand, the constraints in Eqs. (18) and (19) become the following:

$r_{i,t}^{up} \leq (p_{i,t-1} - r_{i,t-1}^{down}) - p_{i,t} + RU_i^{X-Y} z_{i,t-1} + SU_i^{X-Y} \delta_{i,t}^{on}$	$\forall i \in G$ $\forall t = T^*$	(A.29)
$r_{i,t}^{down} \leq p_{i,t} - (p_{i,t-1} + r_{i,t-1}^{up}) - p_{i,t} + RD_i^{X-Y} z_{i,t} + SD_i^{X-Y} \delta_{i,t}^{off}$	$t \in T^{**}$ $t - 1 \in T^{***}$	(A.30)

With  $RU_i^{X-Y}$ ,  $RD_i^{X-Y}$ ,  $SU_i^{X-Y}$ ,  $SD_i^{X-Y}$ ,  $T^*$ ,  $T^{**}$  and  $T^{***}$  defined as in Table A.1.



## References.

- [1] M. Carrión and J. M. Arroyo, "A computationally efficient mixed-integer linear formulation for the thermal unit commitment problem," *IEEE Trans. Power Syst.*, vol. 21, no. 3, pp. 1371–1378, Aug. 2006, doi: 10.1109/TPWRS.2006.876672.
- [2] Y. Fu, M. Shahidehpour, and Z. Li, "Security-constrained unit commitment with AC constraints," *IEEE Trans. Power Syst.*, vol. 20, no. 2, pp. 1001–1013, May 2005, doi: 10.1109/TPWRS.2005.846076.
- [3] P. P. Gupta, P. Jain, S. Sharma, and R. Bhakar, "Reliability-Security Constrained Unit Commitment based on benders decomposition and Mixed Integer Non-Linear Programming," *2017 Int. Conf. Comput. Commun. Electron. COMPTHELIX 2017*, pp. 328–333, Aug. 2017, doi: 10.1109/COMPTHELIX.2017.8003988.
- [4] B. Dipan Biswas, S. Kamalasadana, and S. Paudyal, "A two-stage combined UC-OPF model using mixed integer and semi-definite programming," *2021 IEEE Power Energy Soc. Innov. Smart Grid Technol. Conf. ISGT 2021*, Feb. 2021, doi: 10.1109/ISGT49243.2021.9372168.
- [5] M. Jiang, H. Ge, Q. Guo, and H. Sun, "Network-Constrained AC Unit Commitment Based on Linear Approximation Techniques," *5th IEEE Conf. Energy Internet Energy Syst. Integr. Energy Internet Carbon Neutrality, EI2 2021*, pp. 2980–2985, 2021, doi: 10.1109/EI252483.2021.9713630.
- [6] Y. C. Ho, "An explanation of ordinal optimization: Soft computing for hard problems," *Inf. Sci. (Nij.)*, vol. 113, no. 3–4, pp. 169–192, Feb. 1999, doi: 10.1016/S0020-0255(98)10056-7.
- [7] Y. Nan, Y. Di, Z. Zheng, C. Jiazhan, C. Daojun, and W. Xiaoming, "Research on modelling and solution of stochastic SCUC under AC power flow constraints," *IET Gener. Transm. Distrib.*, vol. 12, pp. 3618–3625, 2018, doi: 10.1049/iet-gtd.2017.1845.
- [8] N. Amjady, S. Dehghan, A. Attarha, and A. J. Conejo, "Adaptive Robust Network-Constrained AC Unit Commitment," *IEEE Trans. Power Syst.*, vol. 32, no. 1, pp. 672–683, Jan. 2017, doi: 10.1109/TPWRS.2016.2562141.
- [9] C. S. Song, C. H. Park, M. Yoon, and G. Jang, "Implementation of PTDFs and LODFs for Power System Security," *J. Int. Counc. Electr. Eng.*, vol. 1, no. 1, pp. 49–53, 2011, doi: 10.5370/jicee.2011.1.1.049.
- [10] J. Guo, Y. Fu, Z. Li, and M. Shahidehpour, "Direct Calculation of Line Outage Distribution Factors," *IEEE Trans. POWER Syst.*, vol. 24, no. 3, p. 1633, 2009, doi: 10.1109/TPWRS.2009.2023273.
- [11] H. Ronellenfitsch, D. Manik, J. Hörsch, T. Brown, and D. Witthaut, "Dual theory of transmission line outages," 2017.
- [12] M. Giuntoli, V. Biagini, and K. Schönleber, "Novel Formulation of PTDF and LODF Matrices for Security Constrained Optimal Power Flow for Hybrid AC and DC Grids," *Proc. 2019 IEEE PES Innov. Smart Grid Technol. Eur. ISGT-Europe 2019*, 2019, doi: 10.1109/ISGTEurope.2019.8905672.
- [13] Á. S. Xavier, F. Qiu, F. Wang, and P. R. Thimmapuram, "Transmission constraint filtering in large-scale security-constrained unit commitment," *IEEE Trans. Power Syst.*,

- vol. 34, no. 3, pp. 2457–2460, May 2019, doi: 10.1109/TPWRS.2019.2892620.
- [14] A. S. Xavier, F. Qiu, and S. Ahmed, “Learning to Solve Large-Scale Security-Constrained Unit Commitment Problems,” *INFORMS J. Comput.*, vol. 33, no. 2, pp. 739–756, Feb. 2019, Accessed: Oct. 11, 2021. [Online]. Available: <https://arxiv.org/abs/1902.01697v2>.
- [15] Y. Yang, Z. Yang, J. Yu, K. Xie, and L. Jin, “Fast Economic Dispatch in Smart Grids Using Deep Learning: An Active Constraint Screening Approach,” *IEEE Internet Things J.*, vol. 7, no. 11, pp. 11030–11040, Nov. 2020, doi: 10.1109/JIOT.2020.2993567.
- [16] N. Yang *et al.*, “Intelligent Data-Driven Decision-Making Method for Dynamic Multisequence: An E-Seq2Seq-Based SCUC Expert System,” *IEEE Trans. Ind. Informatics*, vol. 18, no. 5, pp. 3126–3137, May 2022, doi: 10.1109/TII.2021.3107406.
- [17] A. Porras, S. Pineda, J. M. Morales, and A. Jimenez-Cordero, “Cost-Driven Screening of Network Constraints for the Unit Commitment Problem,” *IEEE Trans. Power Syst.*, vol. 38, no. 1, pp. 42–51, Jan. 2023, doi: 10.1109/TPWRS.2022.3160016.
- [18] J. Wang, M. Shahidehpour, and Z. Li, “Security-constrained unit commitment with volatile wind power generation,” *IEEE Trans. Power Syst.*, vol. 23, no. 3, pp. 1319–1327, 2008, doi: 10.1109/TPWRS.2008.926719.
- [19] D. Bertsimas, E. Litvinov, X. A. Sun, J. Zhao, and T. Zheng, “Adaptive robust optimization for the security constrained unit commitment problem,” *IEEE Trans. Power Syst.*, vol. 28, no. 1, pp. 52–63, 2013, doi: 10.1109/TPWRS.2012.2205021.
- [20] C. Wang and Y. Fu, “Fully parallel stochastic security-constrained unit commitment,” *IEEE Trans. Power Syst.*, vol. 31, no. 5, pp. 3561–3571, Sep. 2016, doi: 10.1109/TPWRS.2015.2494590.
- [21] L. Wu, M. Shahidehpour, and T. Li, “Stochastic security-constrained unit commitment,” *IEEE Trans. Power Syst.*, vol. 22, no. 2, pp. 800–811, May 2007, doi: 10.1109/TPWRS.2007.894843.
- [22] P. Liu, Z. Wu, W. Gu, P. Yu, J. Du, and X. Luo, “A novel acceleration strategy for N-1 contingency screening in distribution system,” *IEEE Power Energy Soc. Gen. Meet.*, vol. 2020-August, Aug. 2020, doi: 10.1109/PESGM41954.2020.9281445.
- [23] S. R. Cominesi, M. Farina, L. Giulioni, B. Picasso, and R. Scattolini, “A Two-Layer Stochastic Model Predictive Control Scheme for Microgrids,” *IEEE Trans. Control Syst. Technol.*, vol. 26, no. 1, pp. 1–13, Jan. 2018, doi: 10.1109/TCST.2017.2657606.
- [24] J. Balasubramanian and I. E. Grossmann, “Approximation to multistage stochastic optimization in multiperiod batch plant scheduling under demand uncertainty,” *Ind. Eng. Chem. Res.*, vol. 43, no. 14, pp. 3695–3713, Jul. 2004, doi: 10.1021/ie030308+.
- [25] G. Morales-España, “Tight MIP Formulations of the Power-Based Unit Commitment Problem,” *Oper. Res.*, 2015.
- [26] G. E. Constante-Flores, A. J. Conejo, and F. Qiu, “AC network-constrained unit commitment via conic relaxation and convex programming,” *Int. J. Electr. Power Energy Syst.*, vol. 134, 2022, doi: 10.1016/j.ijepes.2021.107364.
- [27] D. A. Tejada-Arango, P. Sanchez-Martin, and A. Ramos, “Security constrained unit commitment using line outage distribution factors,” *IEEE Trans. Power Syst.*, vol. 33, no. 1, pp. 329–337, Jan. 2018, doi: 10.1109/TPWRS.2017.2686701.
- [28] G. Morales-España, C. Gentile, and A. Ramos, “Tight MIP formulations of the power-based unit commitment problem,” *OR Spectr.*, vol. 37, no. 4, pp. 929–950, Oct. 2015, doi: 10.1007/s00291-015-0400-4.
- [29] B. Knueven, J. Ostrowski, and J.-P. Watson, “On Mixed Integer Programming

- Formulations for the Unit Commitment Problem,” *INFORMS J. Comput.*, vol. 34, no. 4, pp. 857–876, 2020, doi: 10.1287/ijoc.2019.0944.
- [30] K. Van Den Bergh and E. Delarue, “An improved method to calculate injection shift keys,” *Electr. Power Syst. Res.*, vol. 134, pp. 197–204, May 2016, doi: 10.1016/J.EPSR.2016.01.020.
- [31] M. Shahidehpour, H. Yamin, and Z. Li, *Market Operations in Electric Power Systems: Forecasting, Scheduling, and Risk Management*. Hoboken, New Jersey: John Wiley & Sons, 2002.
- [32] A. J. Ardakani and F. Bouffard, “Prediction of umbrella constraints,” *20th Power Syst. Comput. Conf. PSCC 2018*, Aug. 2018, doi: 10.23919/PSCC.2018.8450586.
- [33] A. J. Ardakani and F. Bouffard, “Identification of umbrella constraints in DC-based security-constrained optimal power flow,” pp. 1–1, Nov. 2014, doi: 10.1109/PESGM.2014.6938802.
- [34] A. Lodi, “The heuristic (dark) side of MIP solvers,” *Stud. Comput. Intell.*, vol. 434, pp. 273–284, 2013, doi: 10.1007/978-3-642-30671-6\_10/COVER.
- [35] J. T. Holzer, Y. Chen, Z. Wu, F. Pan, and A. Veeramany, “Fast Simultaneous Feasibility Test for Security Constrained Unit Commitment,” *IEEE Trans. Power Syst.*, pp. 1–10, 2023, doi: 10.1109/TPWRS.2023.3265269.
- [36] “How do I implement lazy constraints in Gurobi? – Gurobi Help Center.” <https://support.gurobi.com/hc/en-us/articles/360013197972> (accessed Dec. 31, 2022).
- [37] S. Schmitt, I. Harjunkoski, M. Giuntoli, J. Poland, and X. Feng, “Fast Solution of Unit Commitment Using Machine Learning Approaches,” *ENERGYCON 2022 - 2022 IEEE 7th Int. Energy Conf. Proc.*, 2022, doi: 10.1109/ENERGYCON53164.2022.9830191.
- [38] S. Babaeinejadsarookolae *et al.*, “The Power Grid Library for Benchmarking AC Optimal Power Flow Algorithms,” Aug. 2019, doi: 10.48550/arxiv.1908.02788.
- [39] “Data Miner 2.” <https://dataminer2.pjm.com> (accessed Dec. 31, 2022).
- [40] Optimization Gurobi LLC, “Gurobi Optimizer Reference Manual,” 2022. .